Dear ACP Editor:

We have addressed all the comments raised by both reviewers, and incorporated them in the revised manuscript. Please find below our itemized responses to the reviewer's comments.

Thank you very much for your consideration.

Sincerely,
Yang Yang, et al.

COMMENTS TO THE AUTHOR(S)

Impacts of aerosol-radiation interaction on meteorological forecast over northern China by offline coupling the WRF-Chem simulated AOD into WRF: a case study during a heavy pollution event
Manuscript ID: acp-2019-1056
Authors: Yang, et al.

Reviewer 1

General summary

This paper assesses the impact of incorporating aerosol-radiation interactions in the NWP models on surface radiation and weather forecasts during a heavy pollution episode in North China Plain. Hourly AOD fields simulated using WRF-Chem model are fed offline into the radiation schemes of a WRF based NWP system called RMAPS-RT. The inclusion of aerosols in the NWP system reduced overestimation of daytime surface radiation magnitude and budget, and improved forecasts of temperature and wind speed. The results highlight the importance of including aerosols in the NWP system and are interesting. However, the paper lacks detailed evaluation of AOD and PM2.5 (see my specific comments on improving the evaluation part). Additionally, the paper does not discuss whether or not aerosol induced changes in the weather forecast are statistically significant or not. If changes are not statically significant, it may not be

worthwhile to incorporate more realistic aerosol information in the NWP models and just a climatological aerosol representation in the radiation routines may be sufficient. Thus, I recommend major revisions of the paper before publication in ACP.

Response:

We really appreciate the valuable comments. We have made the following changes according to these comments.

More detailed evaluation of simulated AOD against MODIS and CALIPSO satellite-based products were performed and added in the revised manuscript. In addition, we added more quantitative evaluations of $PM_{2.5}$ mass concentrations including spatial distributions of bias, root mean square error, and correlation coefficient for individual sites during pollution and relatively cleaner periods, as well as the time series of hourly averaged observed and simulated $PM_{2.5}$ concentrations over the Henan and Hebei provinces.

To address the issue about the statistically significance of the aerosol induced impacts on weather forecast, we further conducted three sets of 24-hour forecasts for a longer period lasting 27 days (Jan. 13th- Feb. 8th, 2017), with no AOD field (NoAero), climatological AOD fields (ClimAero) and WRF-Chem simulated hourly AOD fields (ChemAero) included, respectively. The results indicated that the simulation with the inclusion of WRF-Chem simulated hourly AOD fields outperformed other two simulations and showed more improvement on the forecast of surface temperature and near surface wind speed than the simulation with climatological AOD fields. These results are in consistent with the conclusions in the current study. Please see more detailed discussion below.

We expect that you will find that your comments have been considered fully and properly in our revised manuscript. Below are our item-by-item responses.

Specific comments

Line 123: change “accessed” to “assessed”.

Response:

Thanks, corrected.

Line 195-196: why RRTMG was not used for WRF-Chem simulations. Are aerosol-radiation interactions turned off purposely in the WRF-Chem simulations?

Response:

Thanks for your insightful comment. The RRTMG scheme was not included in the version 3.3.1 of WRF-Chem, which was applied in the current study and also in our operational system. The aerosol-radiation interactions were turned off in the WRF-Chem simulations. We do understand that the aerosol-radiation interactions could benefit the simulation of $PM_{2.5}$, particularly the peak values. We would include the aerosol-radiation interactions of WRF-Chem in online test in our further research.

Line 203: Why FNL data were used in WRF-Chem experiments and ECMWF data used as met IC/BC in WRF forecast? What is the sensitivity of meteorological parameters to different driving datasets?

Response:

Thanks for your comment. The ECMWF forecast data were adopted as meteorological IC/BC in the operational meteorological forecast system based on WRF, and the meteorological field forecasted by WRF with the inclusion of data assimilation were then input as IC/BC of operational WRF-Chem simulation. In the beginning of the current study, we first tried FNL data for meteorological IC/BC of WRF-Chem forecast and found that the results were reasonable and satisfying, so we did not evaluate the sensitivity of meteorological driving datasets further. According to the colleagues in our Development Testbed Center, the direction of the WRF forecast meteorological parameter biases (e.g. overestimated temperature) are not so sensitive to the initial conditions, as the same direction of biases occur quickly even with assimilated initials that intentionally overcorrect the original biases; thus we assumed the system is more sensitive to certain processes instead of initials in current configurations. We will conduct further detailed research and test about the sensitivity of meteorological parameters to different driving datasets in our future research.

Lines 205-206: Did you run WRF-Chem continuously for 10 days? If yes, did you use any kind of nudging to limit the drift of meteorological fields from the large-scale reanalysis fields?

Response:

Thanks for your comment. We tried without nudging over the plain areas of

northern China during wintertime in our previous study, and found that the simulations of pollutant were reasonable and the drift were acceptable. Thus, we run WRF-Chem continuously for 10 days without nudging in the current study.

Lines 213-214: I do not agree that MODIS AOD retrievals are not available during this episode. I did a quick average AOD plot in Giovanni and the resulting images are shown below in Figures R1 and R2 for both MODIS Terra and Aqua satellites. While AOD is not available everywhere in the domain but I think the datasets is still useful for validation of the model simulated spatial distribution of AOD. I encourage the authors to use Level 2 MODIS AOD retrievals for comparison with WRF-Chem.

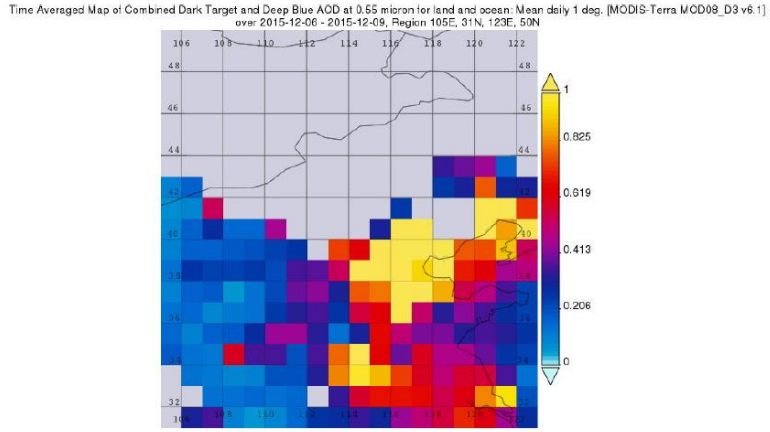

Figure R1: Time averaged MODIS Terra AOD map for 6-9 December 2015.

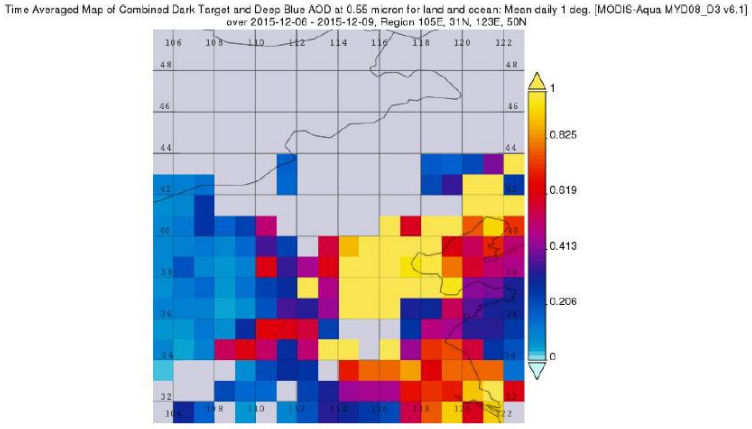

Figure R2: Time averaged MODIS Aqua AOD map for 6-9 December 2015.

Response:

Thanks for your helpful and insightful comment. According to your suggestion, we evaluated the simulated AOD with MODIS Terra and Aqua (Fig. S1). It was seen that WRF-Chem is capable to capture the AOD spatial distribution and also reproduced the transport paths during the event. The simulated high-valued AOD located in Henan on Dec. 6th, then the center moved to Hebei and Beijing on 7th and shifted to northeast areas afterwards. The variations of simulated AOD were in consistent with both Terra and Aqua with slightly overestimated peak value of AOD. In particular, the simulated shifting of AOD center to northeast areas was also observed in Aqua (Fig. S1r-s). We have added the Fig. S1 and the discussion in the revised manuscript (around L247-L255).

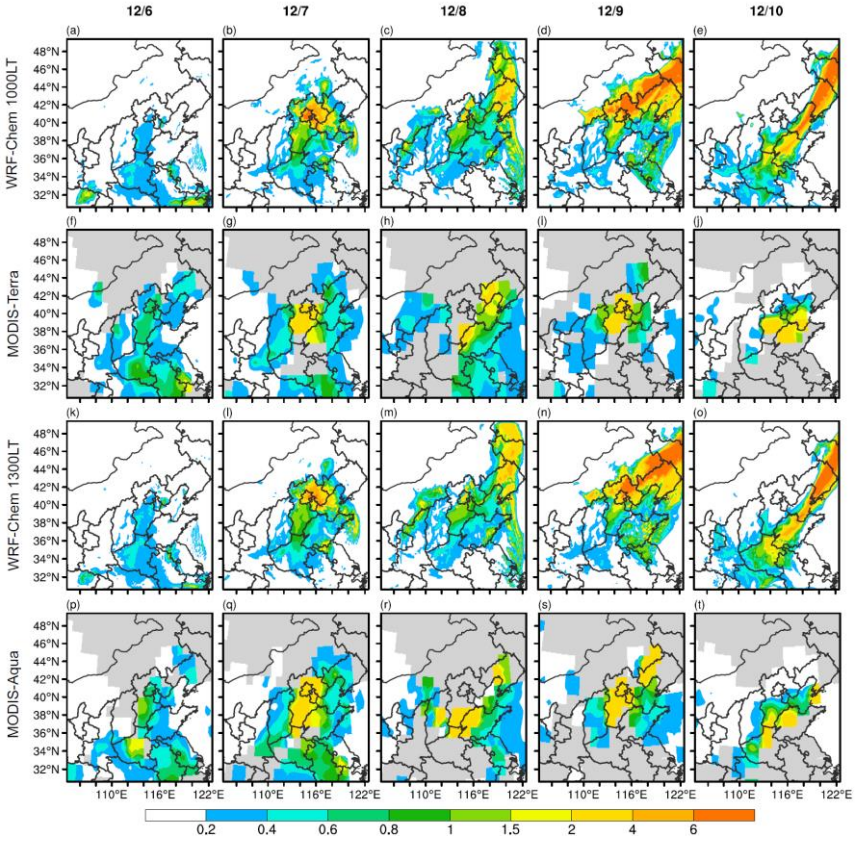

Fig. S1 The WRF-Chem simulated and MODIS observed spatial distribution of AOD on 6th-

10th December (from left to right). The first (a-e) and third rows (k-o) are WRF-Chem simulations at 1000LT and 1300LT (MODIS path times) respectively. The second (f-j) and fourth (p-t) rows are MODIS Terra and Aqua observations, respectively. Gray areas in (f-j) and (p-t) denote the missing values.

Lines 249-250: In addition to my above comment, the authors should consider using other satellite-based products such as MISR and MAIAC AOD, and aerosol extinction coefficient retrievals from CALIPSO.

Response:

Thanks for your helpful and insightful comment. According to your suggestion, we have compared the modeled 550nm aerosol extinction coefficient with CALIPSO, and displayed AOD from MISR level 3 daily product.

Fig. S2 displayed the vertical distribution of simulated 550nm aerosol extinction coefficient compared to those from CALIPSO. Four cross sections along CALIPSO paths on 6th to 9th December were shown. The results indicated that the model could generally reproduce the vertical distribution of extinction coefficients at 550nm in terms of comparable magnitude with those from CALIPSO, particularly on 6th, 7th and 9th, December. However, CALIPSO showed more high values at lower altitude (below 1km) that model failed to capture; the inconsistency may be associated with both CALIPSO retrieval uncertainties at the low altitude and the model itself. We have added the Fig. S2 and the discussion in the revised manuscript (around L255 – L264).

Fig.S3 showed the spatial distribution of AOD at 555nm during 6th to 10th December obtained from MISR. It was seen that the valid fields of AOD from MISR are quite limited during this polluted episode. Therefore, we evaluated the simulation of AOD against MODIS AOD (as discussed earlier) rather than MISR.

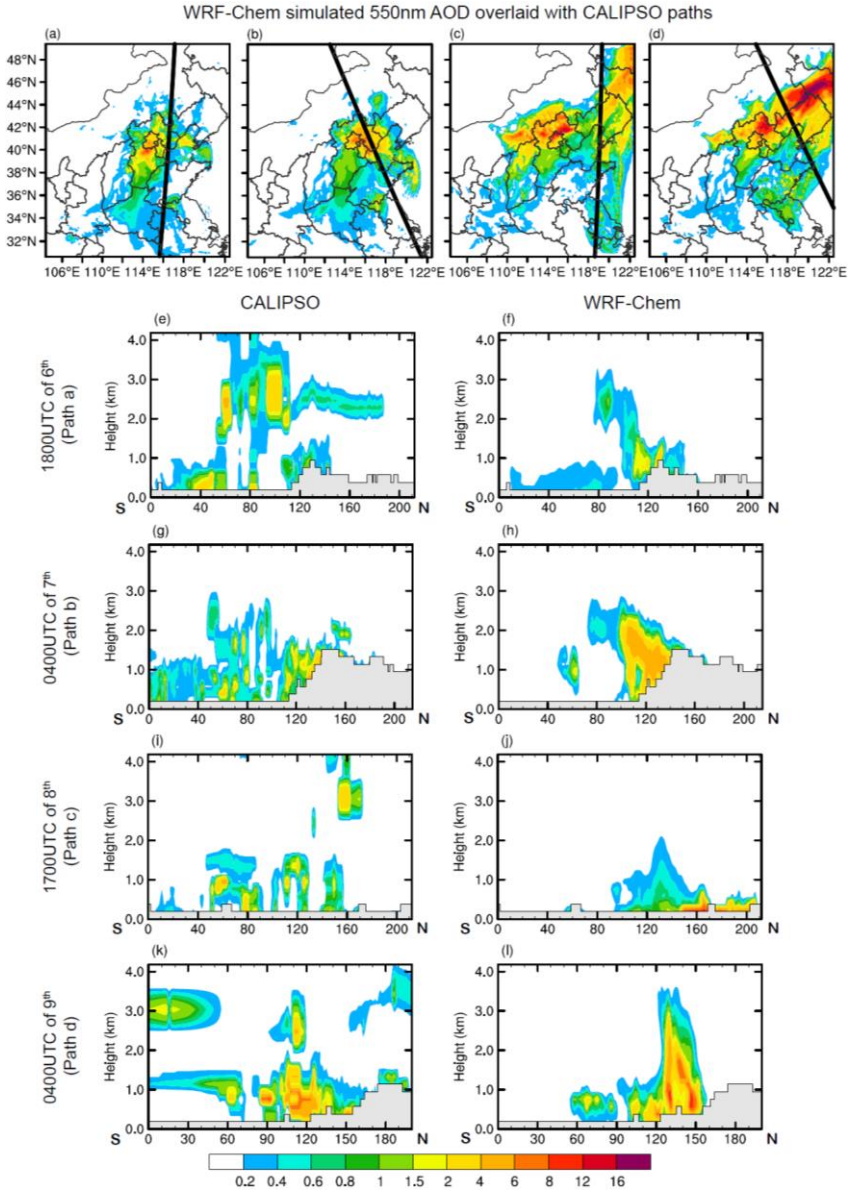

Fig. S2 The WRF-Chem simulated 550nm AOD (shadings) on (a)1800UTC of 6th, (b) 0400UTC of 7th, (c)1700UTC of 8th, (d) 0400UTC of 9th December overlaid with CALIPSO paths (black thick solid). (e-l) denote the corresponding vertical distributions of aerosol extinction coefficient at 550nm from (e, g, i, k) CALIPSO and (f, h, j, l) model simulations. Gray areas in (e-l) denote the terrain.

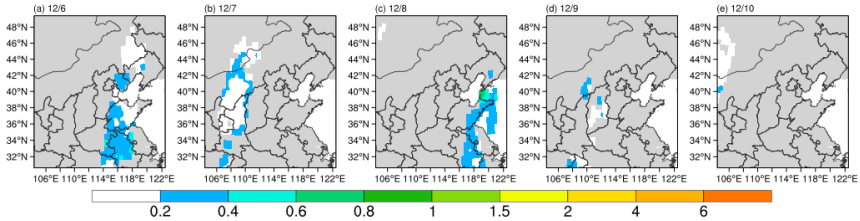

Fig. S3 The spatial distribution of AOD at 555nm from MISR on (a) 6th, (b) 7th, (c) 8th, (d) 9th and (e) 10th December respectively, the gray areas indicate the missing values.

Figure 3 and Lines 253-259: This discussion is very qualitative and I recommend the authors to include some quantitative information about the evaluations. I suggest plotting time series of hourly averaged observed and modeled PM2.5 mass concentrations over the Henen and Hebei provinces (similar to Fig. 4 for the three cities). Maps of bias, root mean square error, and correlation coefficient for each site for the heavy pollution and cleaner periods will also be useful to understand model skill in reproducing the heavy pollution event.

Response:

Thanks for your helpful suggestions. We have added the spatial distributions of bias, root mean square error, and correlation coefficient for individual site during the heavy pollution and relatively cleaner periods (Fig. S4), and the time series of hourly averaged observed and modeled $PM_{2.5}$ mass concentrations over the Henan and Hebei provinces (Fig. 5 d-e).

Figure S4 displayed the mean bias, root mean square error (RMSE), and correlation coefficient during the heavy pollution and relatively cleaner periods. It was seen that the biases of $PM_{2.5}$ were generally less than 40 μg m^{-3} with the correlation coefficient exceeding 0.8 during clean period (Fig. S4a-c). Compared with clean period, the bias and RMSE were generally larger during polluted period (Fig. S4d-f). The $PM_{2.5}$ concentrations over most areas of the domain were underestimated with the maximum bias exceeding 160 μg m^{-3}. Overall, the correlation coefficient was generally higher than 0.4 in northern China during the polluted period, particularly over Beijing with the correlation coefficient reaching 0.8.

To further assess the temporal evolutions of the pollution, the simulated $PM_{2.5}$ concentrations at three major cities (Beijing, Shijiazhuang and Tianjin) and two

provinces (Hebei and Henan) in northern China were compared with observation as shown in Fig. S5. It showed that the hourly variations of $PM_{2.5}$ concentration, including the occurrence of several high peaks at the three cities, as well as the gradual accumulation of pollution in Hebei and Henan could be reasonably reproduced by WRF-Chem. The correlation coefficients (R) between simulation and observation at Beijing, Shijiazhuang, Tianjin, Hebei and Henan were 0.85, 0.89, 0.76, 0.92 and 0.77 respectively. It should be noted that there exits slight overestimation (underestimation) of the peak magnitude during 9th to 10th at Beijing and Shijiazhuang (Tianjin, Hebei and Henan); the overestimation in Beijing and Shijiazhuang is possibly associated with the frequent emission changes caused by emission-control-measures in reality which are not dynamically updated in the model; the underestimation is more related with the deficiency of model skills, such as missing heterogeneous reaction paths in the chemistry scheme.

We have added Fig. S4-5 and the corresponding statement in the revised manuscript around L284-L293 and L294-L308.

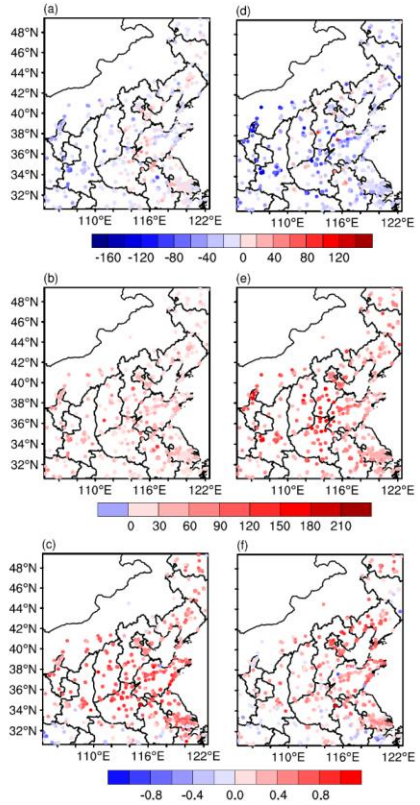

Fig. S4. The (a, d) bias (μg m^{-3}), (b, e) RMSE (μg m^{-3}), and (c, f) correlation coefficient (1) averaged (a-c) during clean period (3^{th} to 5^{th} Dec) and (d-f) the polluted period (6^{th} to 10^{th} Dec).

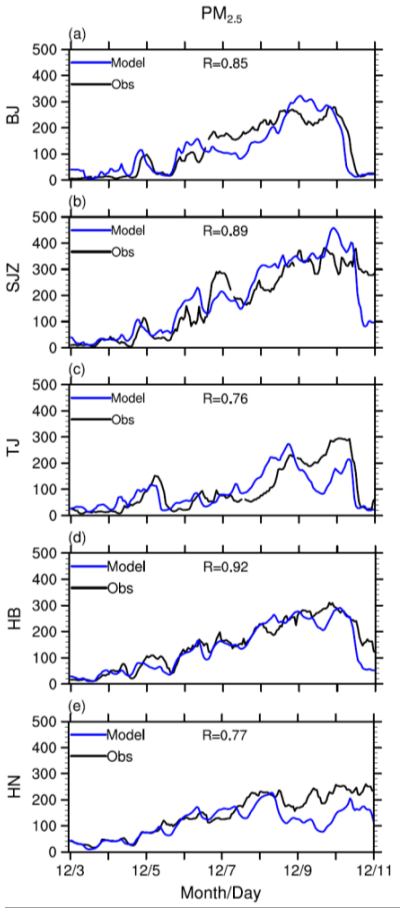

Fig. S5. Observed (black) and WRF-Chem simulated (blue) temporal variation of $PM_{2.5}$ (μg m^{-3}) at three major cities (a) Beijing (BJ), (b) Shijiazhuang (SJZ) (c)Tianjin (TJ) and two provinces (d) Hebei (HB) and (e) Henan (HN).

Line 279: Change “were overlay” to “were overlaid”.

Response:

Thanks, corrected.

Figure 5: Why does the AOD peak before the reduction in SW especially on 6th June? At Taiyuan, there is not much difference between Aero and NoAero simulations which may be because AOD at this site is likely not captured well by the model.

Response:

Thanks for your comment. The pollutant started to accumulate since 6th Dec., accompanied by the increment of AOD. However, the impacts of aerosol-radiation interactions on meteorological fields mainly occurred during daytime through its direct influence on radiation, especially shortwave (SW) radiation. Therefore, the peak timing of reduction in SW may not coincide exactly with that of AOD. In addition, the relation between AOD-induced radiation changes (through aerosol-radiation interaction) and AOD value is not linear.

Line 351: change "biases" to "biased".

Response:

Thanks, corrected.

Line 355: change "leaded" to "led"

Response:

Thanks, corrected.

Line 391: change "shown" to "showed".

Response:

Thanks, corrected.

Section 3.2.2 and related figures: Are the changes in different meteorological parameters statistically significant?

Response:

Thanks for your comment. To addressed this issue, we conducted three sets of 24-hour forecasts for a longer period lasting 27 days (Jan. 13th – Feb. 8th, 2017), with no AOD field (NoAero), climatological AOD fields (ClimAero) and WRF-Chem simulated hourly AOD fields (ChemAero) included, respectively.

The results indicated that the temperature was underestimated (overestimated)

during daytime (nighttime) in NoAero experiment. The temperature is reduced by the aerosol-radiation interactions by inclusion of either climatological or WRF-Chem simulated AOD fields (Fig. S6a), which tends to increase the bias during daytime, and decrease the bias during nighttime. However, the RMSE of temperature in ChemAero is lower than NoAero during the whole 24-hr forecast, particularly at 2000LT of nightfall with the reduction of RMSE reaching ~ 9%. While the RMSE in ClimAero is higher than that in NoAero during daytime (Fig. S6b-c). It is observed in Fig.S7a that, when averaging over Jan. 13th – Feb. 8th, the bias of 2-m temperature in ChemAero (0.48 °C) is lower than those in NoAero (0.79 °C) and ClimAero (0.52 °C). Comparing the absolute bias difference (°C) between ClimAero and NoAero (ClimAero-NoAero), and between ChemAero and NoAero (ChemAero and NoAero) in Fig. S7b, the ChemAero shows more improvement than ClimAero in the simulation of 2m temperature, particularly during the events of Jan. 15-19, and Feb. 3-9. In regards of wind speed at 10m, the overestimated wind speed in NoAero was decreased in ClimAero and ChemAero, with the averaged bias of 1.49 m s $^{-1}$, 1.45 m s $^{-1}$ and 1.44 m s $^{-1}$, respectively (Fig.S7c-d). Moreover, the RMSE in ChemAero was lower than that in ClimAero, particularly during 1700 LT to 0500 LT (Fig.S6e-f). The detailed day-to-day comparisons confirmed the significant temperature improvement by inclusion of WRF-Chem simulated hourly AOD fields during several events, including Jan. 16-19, Jan. 25, Jan. 28, Feb. 3-4, and Feb. 7-9.

Overall, the one-month results are statistically significant which indicated that the simulation with the inclusion of WRF-Chem simulated hourly AOD fields outperformed other two simulations and showed more improvement on the forecast of surface temperature and near surface wind speed than the simulation with climatological AOD fields. We will work on this issue and perform more detailed evaluations and analysis in the future, aiming to facilitate the future inclusion of aerosol-radiation interactions in our regional operational Numerical Weather Prediction system.

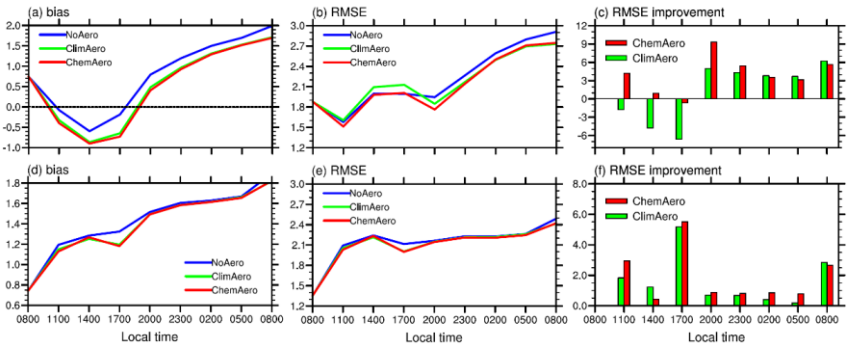

Fig. S6. Area-averaged (a) bias and (b) RMSE of simulated 2-m temperature (°C) in NoAero (blue), ClimAero (green) and ChemAero (red) over NCP area (defined in Fig. 1a), averaged from Jan. 13th – Feb. 8th 2017, and the mean improvement (%) of (c) RMSE in ClimAero (green) and ChemAero (red) relative to NoAero. (d-f) are same with (a-c), but for wind speed at 10m (m s $^{-1}$).

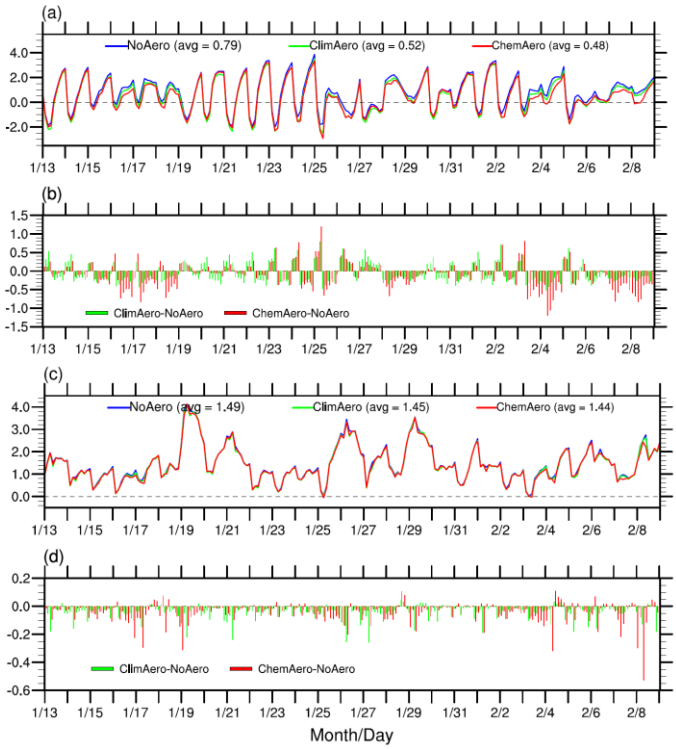

Fig. S7. (a) Temporal variations (00 UTC of Jan. 13th – 24 UTC of Feb. 8th, 2017) of area-averaged 2-m temperature bias (°C) simulated in NoAero (blue soild), ClimAero (green solid)

and ChemAero (red soild) over NCP area (defined in Fig. 1a); (b) same with (a), but for the difference of absolute bias (°C) between ClimAero and NoAero (ClimAero-NoAero, green bars), and between ChemAero and NoAero (ChemAero-NoAero, red bars). (c-d) are same with (a-b), but for wind speed at 10m (m s^{-1}).

Dear ACP Editor:

We have addressed all the comments raised by both reviewers, and incorporated them in the revised manuscript. Please find below our itemized responses to the reviewer's comments.

Thank you very much for your consideration.

Sincerely,
Yang Yang, et al.

COMMENTS TO THE AUTHOR(S)
Reviewer 2

Interactive comment on "Impacts of aerosol-radiation interaction on meteorological forecast over northern China by offline coupling the WRF-Chem simulated AOD into WRF: a case study during a heavy pollution event" by Yang Yang et al.

Angela Benedetti (Referee)
angela.benedetti@ecmwf.int
Received and published: 23 March 2020

General summary

The article is interesting and treats a topic of utmost relevance, that of aerosol impacts on Numerical Weather Prediction (NWP). The authors have analyzed in great detail a pollution case in Northern China during December 2-11, 2015 and examined the impact of including aerosol radiative forcing on several key meteorological variables. They found that aerosols have a large impact on shortwave radiative fluxes at the surface and consequently on 2m temperatures and wind speed using independent observations from various networks to establish that. These results are consistent with finding from other authors who highlighted the importance of a correct inclusion of aerosol fields particularly under extreme aerosol loads.

The paper deserves attention and with some refinements will be acceptable for publication. However, it is worthwhile to stress that case studies such as this may not be statistically significant, especially because extreme aerosol conditions were chosen. It would be necessary to run more cases, possibly entire seasons. I would encourage he authors to get in touch with the rest of the community and join an effort sponsored y WMO via various committees (WGNE, GAW and S2S) to run coordinate experimentation in regional and global models with the goal to gain a fuller picture of the aerosol pacts in NWP. Feel free to contact me directly about this.

Response:

Dear Angela,

We are really glad to be reviewed by you and get to know that different groups are working on this important topic. We will try to get in touch with you and the community in the near future and promote the operational application in our system; in this way, the long-term assessment of aerosol impacts over the northern China region would be possibly conducted routinely, not only confined on the scientific level.

We really appreciate your interest and insightful comments. To address this issue about the statistically significance of the aerosol induced impacts on weather forecast, we further conducted three sets of 24-hour forecasts for a longer period lasting 27 days (Jan. 13th- Feb. 8th, 2017), with no AOD field (NoAero), climatological AOD fields (ClimAero) and WRF-Chem simulated hourly AOD fields (ChemAero) included, respectively.

The results indicated that the temperature was underestimated (overestimated) during daytime (nighttime) in NoAero experiment. The temperature is reduced by the aerosol-radiation interactions by inclusion of either climatological or WRF-Chem simulated AOD fields (Fig. S1a), which tends to increase the bias during daytime, and decrease the bias during nighttime. However, the RMSE of temperature in ChemAero is lower than NoAero during the whole 24-hr forecast, particularly at 2000LT of nightfall with the reduction of RMSE reaching ~ 9%. While the RMSE in ClimAero is higher than that in NoAero during daytime (Fig. S1b-c). It is observed in Fig.S2a that, when averaging over Jan. 13th – Feb. 8th, the bias of 2-m temperature in ChemAero (0.48 °C) is lower than those in NoAero (0.79 °C) and ClimAero (0.52 °C). Comparing the absolute bias difference (°C) between ClimAero and NoAero (ClimAero-NoAero), and between ChemAero and NoAero (ChemAero and NoAero) in Fig. S2b, the

ChemAero shows more improvement than ClimAero in the simulation of 2m temperature, particularly during the events of Jan. 15-19, and Feb. 3-9. In regards of wind speed at 10m, the overestimated wind speed in NoAero was decreased in ClimAero and ChemAero, with the averaged bias of 1.49 m s $^{-1}$, 1.45 m s $^{-1}$ and 1.44 m s $^{-1}$, respectively (Fig.S2c-d). Moreover, the RMSE in ChemAero was lower than that in ClimAero, particularly during 1700 LT to 0500 LT (Fig.S1e-f). The detailed day-to-day comparisons confirmed the significant temperature improvement by inclusion of WRF-Chem simulated hourly AOD fields during several events, including Jan. 16-19, Jan. 25, Jan. 28, Feb. 3-4, and Feb. 7-9.

Overall, the one-month results are statistically significant which indicated that the simulation with the inclusion of WRF-Chem simulated hourly AOD fields outperformed other two simulations and showed more improvement on the forecast of surface temperature and near surface wind speed than the simulation with climatological AOD fields. We will work on this issue and perform more detailed evaluations and analysis in the future, aiming to facilitate the future inclusion of aerosol-radiation interactions in our regional operational Numerical Weather Prediction system.

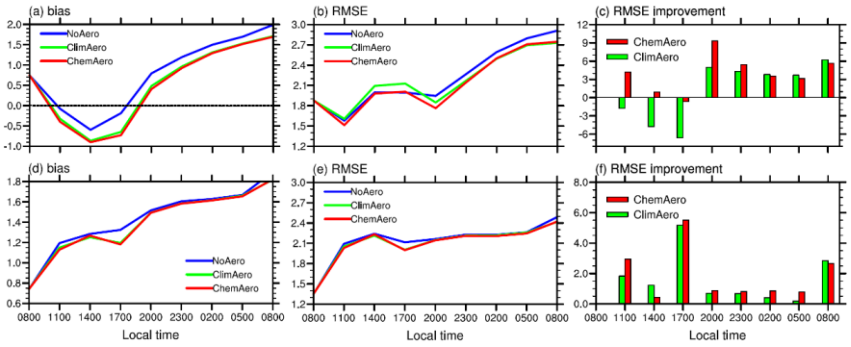

Fig. S1. Area-averaged (a) bias and (b) RMSE of simulated 2-m temperature (°C) in NoAero (blue), ClimAero (green) and ChemAero (red) over NCP area (defined in Fig. 1a), averaged from Jan. 13th – Feb. 8th 2017, and the mean improvement (%) of (c) RMSE in ClimAero (green) and ChemAero (red) relative to NoAero. (d-f) are same with (a-c), but for wind speed at 10m (m s $^{-1}$).

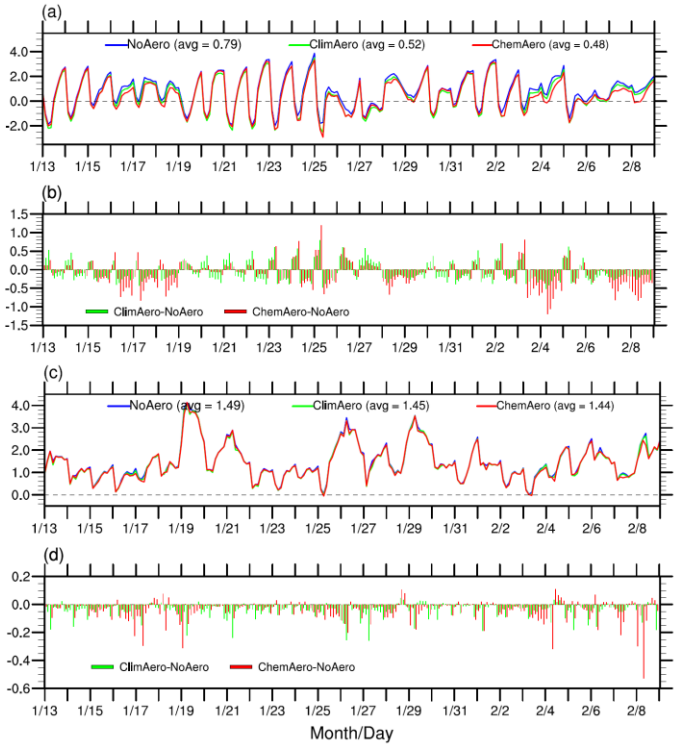

Fig. S2. (a) Temporal variations (00 UTC of Jan. 13th – 24 UTC of Feb. 8th, 2017) of area-averaged 2-m temperature bias (°C) simulated in NoAero (blue soild), ClimAero (green solid) and ChemAero (red soild) over NCP area (defined in Fig. 1a); (b) same with (a), but for the difference of absolute bias (°C) between ClimAero and NoAero (ClimAero-NoAero, green bars), and between ChemAero and NoAero (ChemAero-NoAero, red bars). (c-d) are same with (a-b), but for wind speed at 10m (m s $^{-1}$).

Minor comments and typos

line 22, high-frequency

Response:

Thanks, corrected.

line 66, episodic aerosol events

Response:

Thanks, corrected.

line 105, to facilitate the inclusion of…

Response:

Thanks, corrected.

line 116, was included

Response:

Thanks, corrected.

line 119 For these research studies using operational NWP systems, offline approaches were mostly used. Actually, in Remy et al 2015 and Mulcahy et al 2014 that was not the case and the interactive aerosols were run online.

Response:

Thanks for your comment. We have changed the sentence to "For these research serving for operational NWP systems, both online and offline approaches (that aerosol information were simulated by separate chemistry system and then offline coupled to NWP model) were widely used." In the revised manuscript.

line 143, in an NWP system

Response:

Thanks, corrected.

line 152, future applications

Response:

Thanks, corrected.

line 153, The remainder of the paper is organised: : : Please change all tenses in this paragraph to present.

Response:

Thanks, corrected.

line 168, National

Response:

Thanks, corrected.

line 169, Environmental - please re-run the paper through a spell and grammar checker to ensure that typos are corrected

Response:

Thanks, corrected.

line 171, with a higher

Response:

Thanks, corrected.

line 174 the Rapid Radiative

Response:

Thanks, corrected.

line 181 The RRTMG

Response:

Thanks, corrected.

line 185 was input

Response:

Thanks, corrected.

line 186 integral

Response:

Thanks, corrected.

lie 189 which was - please check that verbs are correctly conjugated

Response:

Thanks, corrected.

line 190 the same configuration

Response:

Thanks, corrected.

line 206 did you investigate the sensitivity of the model AOD to the choice of these ICs and BCs?

Response:

Thanks for the kind reminder! Actually for these heavily polluted region in winter, the initial and boundary conditions are really not so important as in the clean regions, since the pollutant accumulation are usually associated with the high-intensity emission emitted and unfavorable meteorology conditions. For boundary condition, the default profile in WRF-Chem model seemed Okay for this region. For initial conditions, several-days spin-up staring from clean case and going-on for 3-4 days accumulation is usually close enough to real case. We have tried MOZART boundary condition for summer and did see some differences. We may test the sensitivity of the modeled AOD to the choice of chemical ICs and BCs in the future.

line 216 were CARSNET (https://www.atmos-chem-phys.net/15/7619/2015/) observations available over the area? if yes, why were they not used?

Response:

Thanks for your comment. Currently, we don't think the CARSNET dataset is publicly released and we don't have official access to it neither, but we agree with you that the collaboration is helpful in research work. To address the importance of simulated AOD accuracy, we added the evaluations of modeled AOD and aerosol extinction coefficient against MODIS and CALIPSO satellite-based products, respectively.

The modeled AOD was evaluated against MODIS Terra and Aqua (Fig. S3). It was seen that WRF-Chem is capable to capture the AOD spatial distribution and also reproduced the transport paths during the event. The simulated high-valued AOD located in Henan on Dec. 6th, then the center moved to Hebei and Beijing on 7th and shifted to northeast areas afterwards. The variations of simulated AOD were in consistent with both Terra and Aqua with slightly overestimated peak value of AOD. In particular, the simulated shifting of AOD center to northeast areas was also observed in Aqua (Fig. S3r-s).

Fig. S4 displayed the vertical distribution of simulated 550nm aerosol extinction coefficient compared to those from CALIPSO. Four cross sections along CALIPSO paths on 6th to 9th December were shown. The results indicated that the model could generally reproduce the vertical distribution of extinction coefficients at 550nm in terms

of comparable magnitude with those from CALIPSO, particularly on 6th, 7th and 9th, December. However, CALIPSO showed more high values at lower altitude (below 1km) that model failed to capture; the inconsistency may be associated with both CALIPSO retrieval uncertainties at the low altitude and the model itself.

We have added the Fig. S3-4 and the discussion in the revised manuscript (around L247- L255 and around L255-L264).

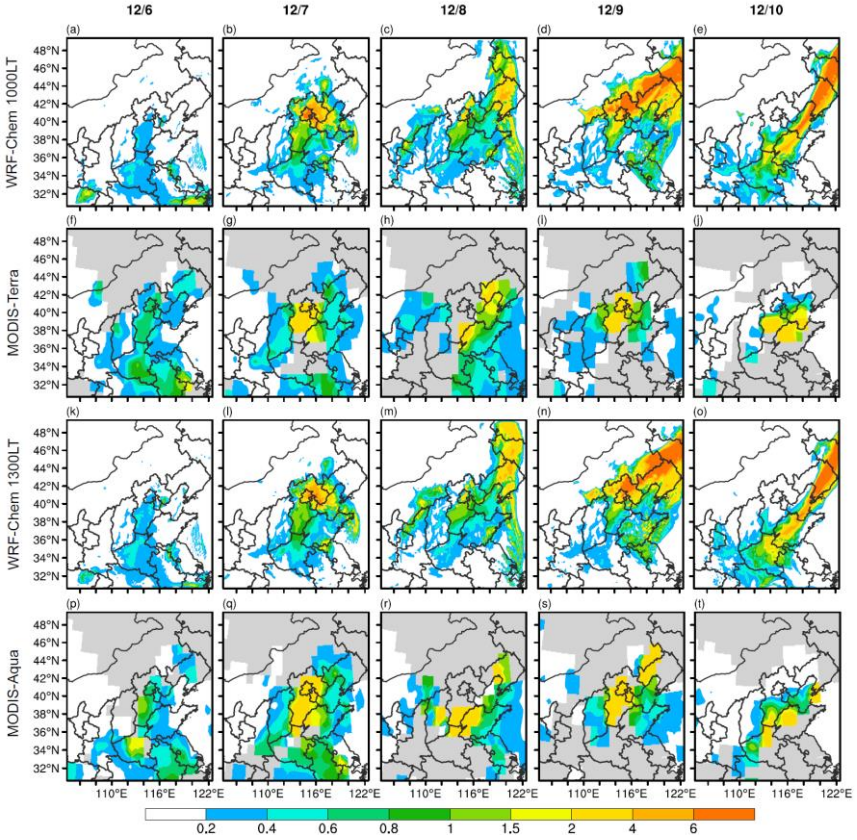

Fig. S3 The WRF-Chem simulated and MODIS observed spatial distribution of AOD on 6th-10th December (from left to right). The first (a-e) and third rows (k-o) are WRF-Chem simulations at 1000LT and 1300LT (MODIS path times) respectively. The second (f-j) and fourth (p-t) rows are MODIS Terra and Aqua observations, respectively. Gray areas in (f-j) and (p-t) denote the missing values.

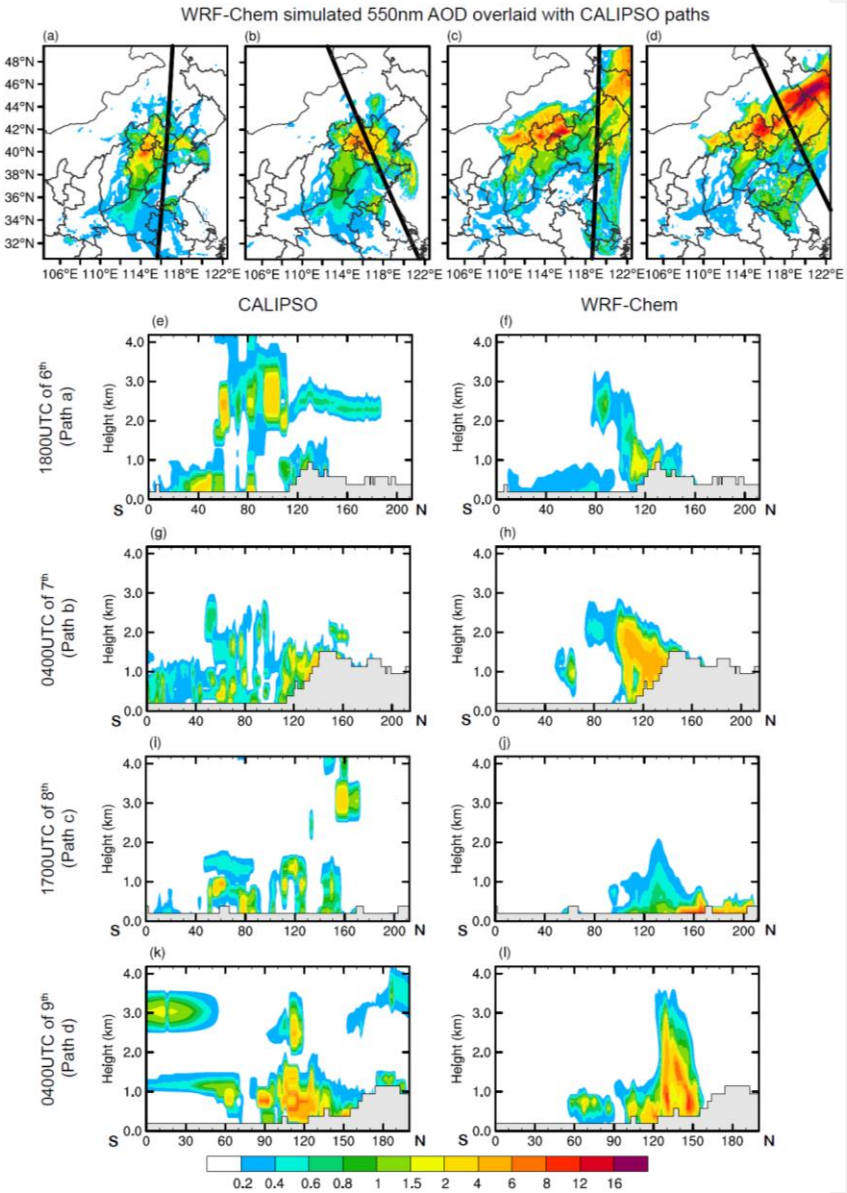

Fig. S4 The WRF-Chem simulated 550nm AOD (shadings) on (a)1800UTC of 6th, (b) 0400UTC of 7th, (c)1700UTC of 8th, (d) 0400UTC of 9th December overlaid with CALIPSO paths (black thick solid). (e-l) denote the corresponding vertical distributions of aerosol extinction coefficient at 550nm from (e, g, i, k) CALIPSO and (f, h, j, l) model simulations. Gray areas in (e-l) denote the terrain.

line 237 / Figure 2 I think it would be good to have extra data from CARSNET if possible

Response:

Thanks for your insightful comment. We added the evaluations of modeled AOD and aerosol extinction coefficient against MODIS and CALIPSO satellite-based products, respectively. Please see more detailed discussion above.

line 244 most of them, do you mean the observations during the peak? See comment above.

Response:

Yes, the observation of AERONET are quite limit during the peak. We added the evaluations of AOD simulation with MODIS and CALIPSO satellite-based products. Please see more detailed discussion above.

line 245 were similar to

Response:

Thanks, corrected.

line 247 you need more observations to establish that

Response:

Thanks, we agree with you that the statement seems arbitrary without more observations here, we have deleted this sentence in the revised manuscript.

line 265 do you think this was because of the emission inventories used or the skill of the model or both? Please comment.

Response:

Thanks for your comment. From our experience, these biases in two directions are related with both the emission inventories used and the skill of the model, but more diagnostic should be conducted to gain solid conclusions. We have added the comment "It was note that there exits slight overestimation (underestimation) of the peak magnitude during 9th to 10th at Beijing and Shijiazhuang (Tianjin, Hebei and Henan);the overestimation in Beijing and Shijiazhuang is possibly associated with the frequent emission changes caused by emission-control-measures in reality which are not

dynamically updated in the model; the underestimation is more related with the deficiency of model skills, such as missing heterogeneous reaction paths in the chemistry scheme." in the revised manuscript.

line 286 In the NoAero experiments were the aerosols completely missing from the simulation or was a climatology used?

Response:

NoAero experiments were the aerosols completely missing from the simulation, we have added the clarification about this issue as "The only difference between the two sets of forecasts is whether the aerosol radiative feedback is activated (Aero, with WRF-Chem simulated hourly AOD fields as input fields) or not (NoAero, no aerosol included), and other schemes remained the same." in the revised manuscript (around L214-L217).

line 302 if a climatology were used would this discrepancy be less severe? I am assuming that in the NoAero simulations there were really no aerosols.

Response:

Thanks for your comment. NoAero experiments were the aerosols completely missing from the simulation, we agree with you that the discrepancy of shortwave radiation would be less severe if a climatological AOD were used.

line 304 this type of bias in SW fluxes is huge

Response:

Thanks for your comment. The polluted episode is a severe event with the maximum of AOD exceeding 8 at Beijing. Therefore, the SW fluxes were profoundly overestimated due to the missing processes of strong forcing from aerosol-radiation interaction, in the NoAero experiment. Actually we suspect the aerosol-cloud interactions may play some role in reality as well.

line 321/Figure 6 At some stations the bias in SW fluxes is not improved as much as in Beijing - do you have an explanation for that?

Response:

Thanks for your comment. The magnitude of changes in SW radiation induced by aerosol-radiation interaction is associated with the magnitude of AOD. The AOD at

Beijing is much higher than those of Tianjin, Taiyuan and Jinan. Therefore, the biases in SW fluxes at these stations were not improved as much as that at Beijing. We have added the discussion about this issue in the revised manuscript (L351-L352).

line 341 are discussed

Response:

Thanks, corrected.

line 368 is this an average value? With the biases in SW radiation being so large I would have expected higher temperature biases.

Response:

Thanks for your comment. The temperature bias is the averaged bias over NCP domain and for the whole period during 6th to 10th December. We have clarified this issue in the revised manuscript.

line 420 / Figure 15, the wind profile at Beijing is quite different from observations in both Aero and NoAero experiments, do you have an explanation for that?

Response:

Thanks for your comment. The wind speed at lower layers is generally overestimated in our operational NWP system, but with much lower magnitude than those shown in Fig. 15. The large bias in Fig. 15 is probably related with the problem about the presentation of boundary layer processes for this period in the model.

line 450 very nice discussion of the impacts on the vertical stratification

Response:

Thanks for your comment.

line 461, please specify if an aerosol climatology was used in NoAero

Response:

Thanks, NoAero experiments were the aerosols completely missing from the simulation, we have clarified this issue in the revised manuscript (L495-L499).

line 520 the fact that aerosol-cloud interactions were not included in the study should be mentioned also at the beginning.

Response:

Thanks, we have added the statement “It is noted that the aerosol-cloud interactions were not included in the study” in the revised manuscript (L217-L218).

1

Impacts of aerosol-radiation interaction on meteorological forecast over northern China by offline coupling the WRF-Chem simulated AOD into WRF: a case study during a heavy pollution event

Yang Yang[1], Min Chen[1], Xiujuan Zhao[1*], Dan Chen[1*], Shuiyong Fan[1], and Shaukat Ali[2]

1 Institute of Urban Meteorology, China Meteorological Administration, Beijing 100089, China

2 Global Change Impact Studies Centre, Ministry of Climate Change, Islamabad 44000, Pakistan

Abstract

To facilitate the future inclusion of aerosol-radiation interactions in the regional operational Numerical Weather Prediction (NWP) system – RMAPS-ST (adapted from Weather Research and Forecasting, WRF) at the Institute of Urban Meteorology (IUM), China Meteorological Administration (CMA), the impacts of aerosol-radiation interactions on the forecast of surface radiation and meteorological parameters during a heavy pollution event (December 6th -10th, 2015) over northern China were investigated. The aerosol information was simulated by RMAPS-Chem (adapted from WRF model coupled with Chemistry, WRF-Chem) and then offline-coupled into Rapid Radiative Transfer Model for General Circulation Models (RRTMG) radiation scheme of WRF to enable the aerosol-radiation feedback in the forecast. To ensure the accuracy of high-~~frequent~~frequency (hourly) updated aerosol optical depth (AOD) field, the temporal and spatial variations of simulated AOD and aerosol extinction coefficient at 550nm were evaluated against in-situ and satellite ~~and in-situ~~ observations~~, which~~. Comparisons with in-situ and Moderate Resolution Imaging Spectroradiometer (MODIS), AErosol Robotic NETwork (AERONET), and Cloud-Aerosol Lidar and Infrared Pathfinder Satellite Observation (CALIPSO) satellite observations showed ~~great consistency~~that the model could reproduce and spatial and vertical distribution as well as the temporal variation the of polluted episode. Further comparison of $PM_{2.5}$ with in-situ observation showed WRF-Chem reasonably captured the $PM_{2.5}$ field in terms of spatial distribution and magnitude, with the correlation coefficients of 0.85, 0.89, 0.76,

0.92 and 0.~~76~~77 at Beijing, Shijiazhuang ~~and,~~ Tianjin, Hebei and Henan, respectively. Forecasts with/without the ~~hourly~~ aerosol information were conducted further, and the differences of surface radiation, energy budget, and meteorological parameters were evaluated against surface and sounding observations. The offline-coupling simulation (with aerosol-radiation interaction active) showed a remarkable decrease of downward shortwave (SW) radiation reaching surface, thus helping to reduce the overestimated SW radiation during daytime. The simulated surface radiation budget was also improved, with the biases of net surface radiation decreased by 85.3%, 50.0%, 35.4%, and 44.1% during daytime at Beijing, Tianjin, Taiyuan and Jinan respectively, accompanied by the reduction of sensible (16.1 W m^{-2}, 18.5%) and latent (6.8 W m^{-2}, 13.4%) heat fluxes emitted by the surface at noon-time. In addition, the cooling of 2-m temperature (~0.40 °C) and the decrease of horizontal wind speed near surface (~0.08 m s^{-1}) caused by the aerosol-radiation interaction over northern China helped to reduce the bias by ~73.9% and ~7.8% respectively, particularly during daytime. Further comparisons indicated that the simulation implemented AOD could better capture the vertical structure of atmospheric wind. Accompanied with the lower planetary boundary layer and the increased atmospheric stability, both U and V wind at 850hPa showed the convergence which were unfavorable for pollutants dispersion. Since RMPAS-ST provides meteorological initial condition for ~~RMPS~~RMAPS-Chem, the changes of meteorology introduced by aerosol-radiation interaction would routinely impact the simulations of pollutants. These results demonstrated the profound influence of aerosol-

radiation interactions on the improvement of predictive accuracy and the potential prospects to offline couple near-real-time aerosol information in regional RMAPS-ST NWP in northern China.

Key words: Aerosol-radiation interactions, offline-coupling, WRF, northern China, pollution

1. Introduction

Aerosol-radiation interactions modify the radiative energy budget of the earth-atmosphere system through the interaction between aerosols and solar radiation by scattering and absorbing mechanism as well as the absorption and emitting of thermal radiation (Ramanathan et al., 2001; Yu et al., 2006). The aerosol-radiation interaction may cool or heat the earth-atmosphere system, alter surface and atmospheric radiation and temperature structure on regional and global climate, which have been widely reported and studied (Hansen et al., 1997; Ramanathan et al., 2001; Kaufman et al., 2002; Liao et al., 2006; Zhang et al., 2010; Ghan et al., 2012; Yang et al., 2017a). Considering the lifetime of most aerosol particles and their locally uneven distribution, as well as their high dependence on emission sources and local meteorological conditions for dispersion (Rodwell and Jung, 2008; Liu et al., 2012; Liao et al, 2015), the impacts of episodic aerosol ~~in short durations~~events over regional areas are worthy of more concerns (Cheng et al., 2017; Zheng et al., 2019).

With substantial aerosol loading, aerosol particles have significant influences on meteorology, and many endeavors by both field experiments and numerical models have been devoted to study the impacts of aerosol-radiation interaction on meteorological fields, including surface solar radiation, planetary boundary layer (PBL), atmospheric heating rate, atmospheric stability (Hansen et al., 1997; Ackerman et al., 2000; Quan et al., 2014; Yang et al., 2017b; Wang et al., 2018), cloud formation due to thermodynamic changes, and further the onset or reduction of precipitation

systems (Grell et al., 2011; Guo et al., 2016). For instance, in worldwide, the simulations with Weather Research and Forecasting (WRF) model coupled with Chemistry (WRF-Chem) showed that by purely taking into account the aerosol-radiation interactions, aerosols may reduce incoming solar radiation by up to -9% (-16%) and 2-m temperatures by up to 0.16°C (0.37°C) in January (July) over the continental U.S. (Zhang et al., 2010) , affect meso-scale convection system owing to thermodynamic changes over Atlantic Ocean during Saharan dust eruption period (Chen et al., 2017), and lead to the distinct changes in precipitation due to the changes in temperature profile and stabilities induced by the aerosol-radiation interaction over Eastern China (Huang et al., 2016).

Northern China is experiencing heavy air pollution in past two decades, with particle matter (PM) being the primary pollutant, particularly during wintertime (Chan and Yao, 2008; Zhang et al., 2015; Zhao et al., 2019) due to the combination of high primary and precursor emissions and frequent stable meteorological conditions in this area (Elser et al., 2016; Zhang et al, 2018). The effects of aerosol-radiation interaction on meteorology were expected to be much more significant over northern China. Applying WRF and Community Multi-scale Air Quality Model (CMAQ) system (WRF-CMAQ), Wang et al. (2014) and Sekiguchi et al. (2018) reported a 53% reduction in solar radiation reaching surface and ~100m decrease of planetary boundary layer height (PBLH) in response to the presence of aerosols during a severe winter haze episode in China. Wang et al. (2015a, b) used the online chemical weather forecasting

mode Global/Regional Assimilation and PrEdiction System/ Chinese Unified Atmospheric Chemistry Environment (GRAPES/CUACE) and illustrated that the solar radiation at ground decreased by 15% in Beijing–TianJin–Hebei, China, and its near surroundings, accompanied by the decrease in turbulence diffusion of about 52% and a decrease in PBLH of about 33 % during a haze episode of summertime in 2008.

Considering the significant influence of the aerosol-radiation interaction on meteorological forecasts as illustrated in many studies (Kaufman et al., 2002; Zhang et al., 2010), several weather forecast centers are conducting research to facilitate the inclusion of more complex aerosol information ~~inclusion~~ in operational numerical weather prediction (NWP) models. For example, Rodwell and Jung (2008) showed the local medium-range forecast skills were improved due to the application of new climatological aerosol distribution in European Centre for Medium-Range Weather Forecasts (ECMWF). Recently, a positive impact up to a 48h lead time on the 2m temperature and forecasts of surface radiative fluxes were reported in ECMWF by applying the prognostic aerosols compared to the monthly climatological aerosol (Rémy et al., 2015). Toll et al. (2016) found that the inclusion of aerosol effects in NWP system was beneficial to the accuracy of simulated radiative fluxes, temperature and humidity in the lower troposphere over Europe. In addition, it was shown that the quality of weather forecasts at UK MET office can be further advanced when the real-time aerosol distribution rather than climatological distribution ~~were~~was included, with the decreased bias of downward SW at surface (-2.79 W m^{-2} vs. -5.30 W m^{-2}) and the

mean sea-level pressure (0.71hPa vs. 0.80hPa) (Mulcahy et al., 2014; Toll et al., 2015). For these research serving for operational NWP systems, both online and offline ~~approach~~approaches (that aerosol information were simulated by separate chemistry system and then offline coupled to NWP model) were ~~mostly~~widely used.

In most previous research-targeted modeling studies over northern China, the aerosol-radiation interaction has been widely ~~accessed in~~assessedin online-coupled meteorology-chemistry models, which might not be practical for NWP purpose. Considering aerosol particles differ by morphology, size and chemical composition, therefore, the numerical treatment of aerosol particles in atmospheric models needs sophisticated method and considerable simplifications, which may bring in more assumptions and uncertainties in online coupling (Baklanov et al., 2014). Moreover, the online simulations require quite high computational costs and could not meet the requirement of efficiency for operational NWP. Grell and Baklanov (2011) illustrated that the offline approach could generate to almost identical results compared to online simulation with the offline-coupling intervals about 0.5-1h. Thus, the computational-economic offline simulation provides a feasible and computationally less demanding approach to include the aerosol-radiation interaction in an operational NWP system. Péré et al. (2011) adopted an offline-coupling between the chemistry-transport model CHIMERE and WRF to study the radiative forcing of high load aerosols during the heat wave of summer in 2003 over Western Europe. Wang et al. (2018) offline implemented the daily AOD from Moderate Resolution Imaging Spectroradiometer (MODIS) to

WRF during a heavy winter pollution at Beijing to study the effect of aerosols on boundary layer. Still, there have been few studies that adopted offline simulation to investigate the impacts of aerosol-radiation interactions over northern China ~~on~~in an NWP system. At Institute of Urban Meteorology, regional operational NWP system–RMAPS-ST (adapted from WRF) and regional air quality model–RMPSA-Chem (adapted from WRF-Chem) were applied operationally. In this study, we investigate the radiative effects of aerosols and their feedbacks on weather forecasting over northern China during a polluted event occurred in winter of 2015, and further potential impacts of changed meteorology to the transport and dissipation of pollution. The simulations were in the configurations of the two systems, aiming at presenting the offline-coupling of the high-frequent real-time aerosol distribution simulated by WRF-Chem and WRF, and evaluating the potential effects of aerosol-radiation interactions on the forecast skills in the RMAPS-ST system for future ~~purpose~~applications.

The remainder of the paper ~~was~~is organized as follows. Section 2 ~~presented~~presents the model configuration and experimental design. In section 3, the model's capabilities in capturing and forecasting the pollution episode ~~were~~are validated with observations first, and impacts of aerosol-radiation interactions on meteorological forecasting over northern China ~~were~~are analyzed further. The final section ~~provided~~provides the concluding remarks.

2. Model description and experimental design

WRF is a state-of-the-art atmospheric modeling system designed for both

meteorological research and NWP. The WRF version 3.8.1 released in August, 2016 was used in this study for a domain covering the northern China with a horizontal resolulation of 9km (222×201 grid points, Fig. 1a), and for 50 vertical levels. The lateral boundary condications (BCs) and initial conditions (ICs) for meteorological variables are provided by the forecast of ECMWF. The major physical schemes include the Assymetric Convective Model Version 2 (ACM2) PBL scheme (Pleim, 2007), the Thompson microphysics without aerosol-aware option (Thompson et al., 2008), the Kain-Fritsch cumulus parameterization (Kain, 2004), and the ~~Natioal~~National Center for ~~Envirometal~~Environmental Prediction, Oregon State University, Air Force, and Hydrologic Research Lab's (NOAH) land-surface module (Chen and Dudhia, 2001; Ek et al., 2003). The landuse data have been reprocessed, ~~which has~~with a higher accuracy and finer classification for urban areas (Zhang et al., 2013) and the urban canopy model (UCM) was not actived.

The shortwave and longwave radiation scheme is the Rapid Radiative Transfer Model for General Circulation Models (RRTMG) (Iacono et al., 2008). The RRTMG scheme is a new version of RRTM added in Version 3.1, and includes the Monte Carlo Independent Column Approximation (MCICA) method of random cloud overlap. A recent intercomparison study showed that the RRTMG had relativlely smaller mean errors in solar flux at the surface and the top of the atmosphere (Oreopoulos et al., 2012) and was considered as recommended WRF configuration for air quality modeling (Rogers et al., 2013). The RRTMG scheme is capable to include the climatological

aerosol data with spatial and temporal variations or an external time varing 3D aerosol input through the option of AER_OPT (Ruiz-Arias et al., 2014). In the present study, the real-time hourly aerosol optical depth (AOD) at 550nm from external files ~~were~~was input into WRF following the second approach. The AOD at 550nm was calculated as the vertical ~~intergration~~integral of extinction coefficients at 550nm from WRF-Chem simulation.

WRF-Chem version 3.3.1 was applied in this study, and the horizontal resolution was 9 km, with 222×201 grid points covering northern China, which ~~were~~was the same ~~as configurions~~configurion of WRF mentioned above. WRF-Chem simulates the formation, transformation and transport processes of both primary and secondary atmospheric pollutants, including gases and PM species (Zhao et al., 2019). Physical parameterizations included single-layer Urban Canopy Model, Noah land-surface, Yonsei University (YSU) PBL, Grell-Devenyi ensemble convection, Thompson microphysics, and RRTM longwave and Goddard shortwave radiation (Chen and Dudhia, 2001; Hong et al., 2006; Grell and Dévényi, 2002; Thompson et al., 2008; Mlawer et al., 1997; Chou and Suarez, 1999). Carbon bond mechanism Z (CBMZ) including comprehensive reactions and alterable scenarios were used as the gas-phase mechanism. Model for Simulating Aerosol Interactions and Chemistry (MOSAIC) are used with four size bins (Zaveri and Peters, 1999). Anthropogenic emission data were from the MEIC (2012) inventory (http://www.meicmodel.org/) with a resolution of 0.1 °×0.1 °. Meteorological ICs and BCs were obtained from the Final Analysis data

(FNL) with a resolution of 1.0 °×1.0 ° from the National Centers for Environmental Prediction (NCEP). To generate aerosol fields for study period (Dec. 2nd-11th), 9-days WRF-Chem simulations from Dec. 2nd were conducted using prescribed idealized profiles as ICs and BCs for chemical species.

To estimate the aerosol radiative forcing and its feedbacks on meteorological fields, two sets of 24-hour WRF forecasts were conducted at 00UTC from 2nd-10th December 2015~~ with WRF-Chem simulated AOD fields as input fields~~. The only difference between the two sets of forecasts is whether the aerosol radiative feedback is activated (Aero, with WRF-Chem simulated hourly AOD fields as input fields) or not (NoAero, no aerosol included), and other schemes remained the same. It is noted that the aerosol-cloud interactions were not included in the study.

The sites of observations over simulated domain and northern China plain (NCP, purple box in Fig. 1a) ~~are~~were shown in Fig. 1. ~~Since the~~The 550nm AOD ~~provided by~~ retrievals from Level 2 of MODIS ~~instruments on board NASA~~sensors onboard polar orbiting satellites ~~Aqua and~~ Terra ~~are both not available in the region~~and Aqua satellites were adopted to evaluate the spatial distribution of modeled AOD. The vertical distribution of aerosol extinction coefficient at 550nm were compared with ~~high pollution~~that from Cloud-Aerosol Lidar and Infrared Pathfinder Satellite Observations (CALIPSO) satellite. Moreover, three sites of AErosol Robotic NETwork (AERONET) ~~are~~were used to validate the simulation (black dots in Fig. 1b), and the observed AOD obtained from observation at the Institute of Atmospheric Physics (IAP), Chinese

Academy of Sciences (39°58′ 28″ N, 116°22′ 16″ E) in Beijing city (blue dot in Fig. 1b) ~~is~~was also included as supplementary. The hourly observed $PM_{2.5}$ concentrations of total 813/332 monitoring stations over the study domain/NCP were from the released data by the China National Environmental Monitoring Centre (http://106.37.208.233:20035/, colored dots in Fig. 3a). For given cities (dots in Fig. 1a), hourly $PM_{2.5}$ concentration was represented by the average of data from all monitoring sites located in the city. Simulated meteorological variables including 2-m temperature and wind speed at 10m were evaluated using in-situ observations from National Meteorological Information Center (http://data.cma.cn/data/cdcindex.html) of China Meteorological Administration (CMA, dots in Fig. 8a). The radiations were observed at IAP and in-situ stations of CMA (shown as triangles in Fig. 1a). The vertical observation of atmospheric wind speed from sounding were also used (circles in Fig. 1a). The variables, sources, numbers of sites in the domain and NCP and the frequency of chemical and meteorological observations were also listed in Table 1.

3. Results

3.1 Evaluation of AOD and $PM_{2.5}$ simulated by WRF-Chem

Before the offline-coupling of the WRF-Chem simulated hourly AOD to meteorological model WRF, we first validated the simulated AOD and ensured the model's capability to reproduce the features of the aerosol field. ~~Figure 2~~Figure 2 shows the spatial distribution of modeled AOD and AOD from MODIS Terra and Aqua. It was seen that WRF-Chem is capable to capture the AOD spatial distribution and also

reproduced the transport paths during the event. The simulated high-valued AOD located in Henan on Dec. 6th, then the center moved to Hebei and Beijing on 7th and shifted to northeast areas afterwards. The variations of simulated AOD were in consistent with both Terra and Aqua with slightly overestimated peak value of AOD. In particular, the simulated shifting of AOD center to northeast areas was also observed in Aqua (Fig. 2r-s). To further verify the vertical distribution of aerosol extinction coefficient, Fig. 3 displayed the vertical distribution of simulated 550nm aerosol extinction coefficient compared to those from CALIPSO. Four cross sections along CALIPSO paths on 6th to 9th December were shown. The results indicated that the model could generally reproduce the vertical distribution of extinction coefficients at 550nm in terms of comparable magnitude with those from CALIPSO, particularly on 6th, 7th and 9th, December. However, CALIPSO showed more high values at lower altitude (below 1km) that model failed to capture; the inconsistency may be associated with both CALIPSO retrieval uncertainties at the low altitude and the model itself. Figure 4 further displayed the temporal variation of simulated AOD at 550nm (blue solid) at four sites, in comparison with three AERONET stations (black circles in Figs. ~~2a~~4a-c) and IAP site (black circles in Fig. ~~2d~~4d) for the period during 3rd to 11th ~~Dec~~December, 2015 (local time, LT). As shown in blue solids in Fig. ~~2a~~4a, the simulated AOD increased since 6th Dec. and reached the peak value of 9 on 7th, and the high AOD value maintained until 9th and reached the second peak. The second peak was also observed from AERONET though most of them were missing during the

pollution event. The temporal variations of AOD at Beijing-CMA and IAP (Figs. ~~2b~~4b and d) were ~~analogical with~~similar to those at Beijing station (Fig. ~~2a~~4a). Meanwhile, the simulated AOD at Xianghe (Fig. ~~2c~~4c) was relatively lower than those at other stations~~; it might be that Xianghe is a rural station and was less polluted than urban station during this episode~~.

Considering that ~~the available observational AOD data was quite limited, and~~ the aerosol extinction was mainly attributed to scattering and absorption of solar radiation by $PM_{2.5}$ and their hygroscopic growth with relative humidity (Cheng et al., 2006), next we compared the simulated $PM_{2.5}$ concentrations with corresponding in-situ observation over the model domain. As shown in Fig. ~~3~~5, the simulated and observed pollution were both initiated over Henan province on 6th, further intensified and shifted northward afterwards. The polluted center located over south of Hebei province and maintained until 10th, with the maximum $PM_{2.5}$ concentration exceeding 440μg m^{-3}. The results indicated that WRF-Chem could well capture the spatial features of $PM_{2.5}$ and its temporal variation, in spite of the slight discrepancy of the center position during 9th and 10th. Figure 6 displayed the mean bias, root mean square error (RMSE), and correlation coefficient during the heavy pollution and relatively cleaner periods. It was seen that the biases of $PM_{2.5}$ were generally less than 40 μg m^{-3} with the correlation coefficient exceeding 0.8 during clean period (Fig. 6a-c). Compared with clean period, the bias and RMSE were generally larger during polluted period (Fig. 6d-f). The $PM_{2.5}$ concentrations over most areas of the domain were underestimated with the maximum

bias exceeding 160μg m^{-3}. Overall, the correlation coefficient was generally higher than 0.4 in northern China during the polluted period, particularly over Beijing with the correlation coefficient reaching 0.8.

To further assess the temporal evolutions of the pollution, the simulated $PM_{2.5}$ concentrations at three major cities (Beijing, Shijiazhuang and Tianjin, shown as black dots in Fig. 1a) and two provinces (Hebei and Henan) in northern China were compared with ~~those~~ observation as shown in Fig. ~~4~~7. It showed that the hourly variations of $PM_{2.5}$ concentration, including the occurrence of several high peaks at the three cities, as well as the gradual accumulation of pollution in Hebei and Henan could be reasonably reproduced by WRF-Chem~~, despite the slight overestimation (underestimation) of the peak magnitude during 9th to 10th at Beijing and Shijiazhuang (Tianjin).~~. The correlation coefficients (R) between simulation and observation at Beijing, Shijiazhuang ~~and~~, Tianjin, Hebei and Henan were 0.85, 0.89 ~~and~~, 0.76, 0.92 and 0.77 respectively. It should be noted that there exits slight overestimation (underestimation) of the peak magnitude during 9th to 10th at Beijing and Shijiazhuang (Tianjin, Hebei and Henan); the overestimation in Beijing and Shijiazhuang is possibly associated with the frequent emission changes caused by emission-control-measures in reality which are not dynamically updated in the model; the underestimation is more related with the deficiency of model skills, such as missing heterogeneous reaction paths in the chemistry scheme.

3.2 Aerosol effects on meteorological simulations

In this section, the influences of aerosol-radiation interaction on the spatial and temporal variations of radiation and energy budget simulated by WRF model were analyzed, and their impacts on the forecasts of meteorological fields were discussed further.

3.2.1 Aerosol impacts on simulations of radiative forcing and heat fluxes

To illustrate the impacts of aerosol-radiation interaction on the forecasts of radiation during the pollution event, the simulated surface downward SW radiation and net radiation at Beijing, Tianjin, Taiyuan and Jinan, as denoted by the triangles in Fig. 1a, were compared with observations in Fig. ~~5~~8. To show the relationship with aerosol, the time series of AOD for Dec. 3th -11th were ~~overlay~~overlaid as gray shadings in Fig. ~~5~~8. During the clean stage with quite low AOD values (close to 0) before 6th Dec., both simulations with and without aerosols reasonably reproduced the temporal variation of downward SW at Beijing despite the slightly overestimation during the noon-time (Fig. ~~5a~~8a). However, the overestimated downward SW in NoAero turned to intensify extensively since 6th Dec. and sustained till 10th Dec., accompanied by the occurrence of the pollution with the high AOD value. Meanwhile, the downward SW was much lower in Aero than that in NoAero due to aerosol extinction, with resembled temporal variations and comparable magnitude at the peak time compared to the observations. Similarly, the variations of downward SW from Aero simulation were also closer to observations at Tianjin, Taiyuan and Jinan than those in NoAero (Figs. ~~5b~~8b-d). It was noted that the most significant improvement of simulated downward SW at Jinan

appeared on 10th Dec. and was later than that at Beijing, which was consistent with the AOD's variations at Jinan. Moreover, the surface energy balance was also affected by the reduction of downward SW radiation reaching the ground due to the presence of aerosol particles. As shown in Figs. ~~5e~~8e–h, in corresponding to the changes in downward SW, the variations of net radiation at surface in Aero were also in better agreement with observation during the polluted period than in NoAero, particularly during daytime with the high AOD values.

To further quantify the influence of the aerosol-radiation interaction on the diurnal variation of surface radiation, next we compared the simulated averaged diurnal variation of downward SW and net radiation during the polluted episode (6th to 10th) with observation. Figure ~~6a~~9a showed that there existed a large overestimation of surface downward SW during the daytime in NoAero. Particularly, the overestimated downward SW tented to increase since morning (0800 LT) and peak at noon (1300 LT) with the maximum bias reaching 226.5 W m^{-2}, and the mean bias of ~149.4 W m^{-2} during daytime (averaged during 0800 to 1800 LT, Table 2). However, the overestimated SW radiation was remarkably reduced in Aero with the mean bias of 38.0 W m^{-2} during daytime. Similarly, the diurnal variation and magnitude of downward SW radiation at surface were also better captured at Tianjin, Taiyuan and Jinan in Aero (Figs. ~~6b~~9b–d), with the lower bias (70.9 W m^{-2}, 118.3 W m^{-2} and 97.7 W m^{-2}) than in NoAero (115.5 W m^{-2}, 155.0 W m^{-2} and 149.1 W m^{-2}) during daytime. Note the biases of SW radiation in Tianjin, Taiyuan and Jinan were not improved as much as in Beijing

due to the lower AOD. Consistent with this finding, the reduction of downward SW was also reported in United States (Zhang et al., 2010) and Europe (Toll et al., 2016) with relatively lower decrease (10 W m^{-2} and 18 W m^{-2}); the relatively larger reductions (30-110 W m^{-2}) in northern China is possibly due to the higher aerosol load. Figures ~~6e~~9e–h presented the diurnal variations of net radiation, with positive (negative) net radiation during daytime (nighttime) in observation, and the NoAero tended to overestimate (underestimate) the net radiation at surface during daytime (nighttime), indicating that there existed surplus energy income and outcome in model than those in observation, inducing the larger magnitude of diurnal cycle of net radiation. By including the aerosol-radiation interaction in the model, the simulated diurnal variations of net radiation were markedly improved, particularly during daytime with the reduction of bias by 85.3%, 50.0%, 35.4%, and 44.1% at Beijing, Tianjin, Taiyuan and Jinan, respectively.

In response to the decrease of downward SW radiation and net radiation at the ground during daytime, the surface fluxes also changed in presence of aerosol extinction within the energy-balanced system. Figure ~~7~~10 displayed the difference of surface sensible and latent heat flux between Aero and NoAero at 1300LT, when the influences of the aerosol on radiation reaching the peak. Comparing to the NoAero simulation, both the surface sensible and latent heat flux emitted by the surface were reduced in the Aero simulation, with the domain-average of 16.1 W m^{-2} (18.5%) and 6.8 W m^{-2} (13.4%) respectively. It was noted that the decrease of the surface latent heat

flux was less pronounced than that of surface sensible heat flux, suggesting the impact of aerosol-radiation interaction on the humidity was less significant than that of temperature, which was also reported over United States (Fan et al., 2008) and western Europe (Péré et al., 2011).

3.2.2 Aerosol impacts on simulations of temperature, PBLH and wind fields

The changes in radiation and energy budget through the impacts of aerosol-radiation interaction would certainly induce the changes in PBL thermodynamics and dynamics, which would result in changes in the forecasts of meteorological fields. The impacts on the forecasts of 2-m temperature, PBLH and wind fields due to the aerosol-radiation interaction ~~were~~are discussed in the following subsection.

Figure ~~8~~11 presented the diurnal variation of averaged bias of 2-m temperature during polluted period in NoAero (upper panel) and Aero (lower panel) compared with the in-situ observation during 1100 LT to 2300 LT. It was obvious that the temperature of NoAero was significantly overestimated for a wide range over northern China, particularly over the plain areas including south of Hebei, Henan and Shanxi provinces. The warm biases tended to intensify in the afternoon and reach ~3°C over south part of Hebei province (Figs. ~~8b~~11b–c). Accompanied by the warm ~~biases~~biased over plain areas throughout the day, the mountain areas were dominated by the cold biases until 1700 LT, and turned to be warm biases afterwards, which were attributed by the frozen water in soil due to wet bias of soil moisture over mountain areas, inducing overestimated energy transport from atmosphere to soil during daytime. Compared to

NoAero, the lower temperature in Aero due to the decreased surface solar radiation, caused by aerosol extinction ~~leaded~~led to the reduced warm bias in NCP region. However, the cold bias in Beijing area was slightly intensified, which may partly relevant with the overestimated $PM_{2.5}$ concentration in Beijing and can be improved by incorporating more accurate aerosol information in the future. It was noted that the cold biases over mountain areas associated with the model physics deficiency can not be corrected by aerosol-radiation effects, thus the correction of aerosol-radiation effect may get complex results and differ with regions due to the model pre-existing deficiencies.

To quantitatively evaluate the agreement of simulated 2-m temperature with observations, the mean bias and ~~root mean square error (~~RMSE~~)~~ were employed, and their averaged diurnal variations during the polluted episode (6^{th} to 10^{th}, Dec.) averaged over NCP, denoted by the purple box in Fig. 1a, were displayed in Fig. ~~9~~12. As shown in Fig. ~~9a~~12a, the warm bias in NoAero sustained during the entire 24-hr forecast, ranging from 0.3 °C to 0.9 °C. Compared to NoAero, the NCP area-averaged warm bias was remarkably reduced by ~0.40°C (~73.9%) due to aerosol-radiation interaction, with the maximum reaching ~0.54 °C (~95.0 %) at 1100 LT (Figs. ~~9a~~12a and c). Consistently with mean bias, the RMSE was also lower in Aero than NoAero, particularly during 1100 to 2000 LT during the daytime (Figs. ~~9b~~12b and d).

The aerosol-radiation interaction may also have profound impacts on atmospheric structure in addition to radiation and temperature (Rémy et al., 2015). PBLH is one of

the key parameters to describe the structure of PBL and closely related to air pollution. It was indicated that the mean daytime PBLH over northern China were around 300–600m (Fig. ~~10a~~13a), and declined generally 40–200m (10%–40%) in Aero over the region with highest $PM_{2.5}$ concentration, particularly over Beijing, Tianjin and Hebei (Figs. ~~10b~~13b–c). As shown in dashed lines in Fig. ~~11~~14, the NCP area-averaged PBLH at noon-time (1400 LT) was diminished dramatically by aerosol-radiation interaction during the pollution event over northern China, with the maximum decrease reaching -155.2m on 7th Dec. The reduction of PBLH could be the consequence of more stable atmosphere in Aero than NoAero, which was induced by the terrestrial cooling in the lower part of the planetary boundary layer and the solar heat due to the absorbing in the upper layers (solid lines in Fig. ~~11~~14).

The near surface wind fields changes due to aerosol-radiation interaction were further investigated. Figure ~~12~~15 shows the wind vector in NoAero (upper panel), Aero (middle panel) and their difference (lower panel). It can be seen from Fig. ~~12a~~15a-e that the northern China was dominated by the anticyclonic circulation, accompanied by the relatively weaker northeast wind over Beijing and Hebei areas. The comparisons of Aero and NoAero (Figs. ~~12~~15 k-o) ~~shown~~showed that the northeast wind was increased with the maximum reaching 1 m s^{-1} by aerosol-radiation interaction over Beijing and Hebei, where high particles concentration located (shadings in Figs. ~~12~~15 f-j). Figures ~~12k~~15k-o also indicated the changes of west wind over the south part of the domain and southeast wind over the ocean areas, which tended to weaken the anticyclonic

circulation and thus declined the wind speed there. The reduced wind speed due the inclusion of aerosol-radiation interaction was possible due to the thermal-wind adjustment in response to the more stable near-surface atmosphere, which was also addressed in previous work using WRF-Chem (Zhang et al., 2015).

The comparisons between simulated wind speeds against in-situ observation averaged during 6th to 10th Dec. were displayed in Fig. ~~13~~16. In regard of NoAero, the simulated wind speed at 10m was overestimated over the nearly whole domain with the maximum bias up to 3 m s^{-1} except some mountain sites (upper and middle panels in Fig.~~13~~16). It might be due to the omission of UCM model as the overestimation is more prominent in city clusters (especially in Beijing and southern Hebei) than other areas. Figures ~~13k~~16k-o showed the difference of absolute value of bias between Aero and NoAero and indicated the bias of simulated wind speed were decreased over south and northeast part of the domain during afternoon (Figs. ~~13k~~16k-m) by aerosol-radiation interaction, while were increased over Beijing and Hebei area particularly during nightfall (Fig. ~~13n~~16n) due to the intensified wind speed there. The NCP area-averaged bias and RMSE of wind speed at 10m were further shown in Figure ~~14~~17. It was seen that the aerosol-radiation interaction helped to reduce the overestimation of wind speed at 10m up to 0.08 m s^{-1} (~7.8%), particular during daytime (Figs. ~~14a~~17a and c). Correspondingly, the RMSE of Aero was also lower than that of NoAero, indicating that the inclusion of aerosol-radiation interaction helped to improve the prediction of near surface wind speed on the domain-averaged scale.

Although the changes of wind speed ~~is~~are less straightforward than that of radiation, the aerosol-radiation interactions can also affect dynamic fields (vertical wind shear) through the changes of atmospheric thermal structure and the thermal wind relation when the interaction lasts long enough (Huang et al., 2019). Figure ~~15~~18 displayed vertical profiles of wind speed at the stations of Beijing and Xingtai in simulation and verified with sounding observations. It was shown that the NoAero underestimated (overestimated) the low levels wind speed at 0800 LT (2000 LT) at both Beijing and Xingtai. However, the wind speed ~~were~~was increased (decreased) at 0800 LT (2000 LT) in Aero relative to NoAero, indicating the positive impacts on the simulation of atmospheric winds by aerosol-radiation interaction.

Since the forecast meteorological fields by WRF (RMPAS-ST) is routinely applied to WRF-Chem (RMAPS-Chem) as meteorological ICs in the air quality operational system at IUM, the changed meteorology due to aerosol-radiation interaction will further influence the forecast of pollution through meteorological ICs. In regard of further feedback of aerosol-radiation interactions to the transport and dissipation of the pollutants, their impacts on wind field at 850hPa were further discussed as it is strongly correlated with haze formation (Zhang et al., 2018; Zhai et al., 2019). Figures ~~16~~19 a-e display that northern China was dominated by the anticyclone circulation at 850hPa, associated with the southwest (northwest) wind in the west (east) of the northern part of the domain. The difference of U (zonal, eastward is positive) winds between Aero and NoAero (middle panel in Fig. 16) showed that the U wind was intensified over west

Hebei, accompanied by the quite small changes in Beijing area, indicating that the increased U wind was blocked by the mountains and could not transport the pollutants over Hebei and Beijing to the east (Figs. ~~16~~19 f-h). On the other hand, the changes of V (meridional, northward is positive) show different patterns over north and south of the 38° N (lower panel in Fig. ~~16~~19). In the south part, the increased northward wind due to aerosol-radiation interaction may help to transport pollutants from highly polluted areas to Hebei and Beijing. In the north of the domain, the negative (positive) changes of V wind indicated the reduced northward (southward) wind in west (east) of Hebei, which could suppress the diffusion of the pollutants. As a result, both U and V changes induced by the aerosol-radiation interaction will prevent pollutants from dispersing and may exacerbate the pollution in Heibei and Beijing, which confirms the more stable boundary layer due to aerosol-radiation interaction as discussed earlier.

4. Concluding remarks

To facilitate the future inclusion of aerosol-radiation interactions in the regional operational NWP system – RMAPS-ST (adapted from WRF) at IUM, CMA, the impacts of aerosol-radiation interactions on the forecast of surface radiation and meteorological parameters during a heavy pollution event (Dec. 6^{th} -10^{th}, 2015) over northern China were investigated. The aerosol information (550-nm AOD 2D field) were simulated by WRF-Chem and then offline-coupled into RRTMG radiation scheme of WRF to enable the aerosol-radiation feedback in the forecast. Two sets of 24-hour forecasts were performed at 00UTC from Dec. 2^{nd}-11^{th}, 2015. The only difference

between the two sets of forecasts was whether the aerosol radiative feedback was activated (Aero, with WRF-Chem simulated hourly AOD fields as input fields) or not (NoAero, no aerosol included), while the other schemes remained the same.

The capability of WRF-chem to reproduce the polluted episode was confirmed first before the offline-coupling of AOD to WRF. ~~The~~The validation of simulated AOD and aerosol extinction coefficient against MODIS and CALIPSO confirmed that the model could reproduce both the spatial and vertical distribution of 550nm AOD. Further results indicated that the temporal variations of simulated AOD at 550nm was in consistent with AERONET and in-situ observation at IAP. ~~Furthermore~~In addition, the spatial distributions of $PM_{2.5}$ as well as their magnitude, particularly during the peak stage (8^{th} to 9^{th}) of the pollution event were reasonably captured by WRF-Chem, with the correlation coefficients of 0.85, 0.89, 0.76, 0.92 and 0.~~76~~77 at Beijing, Shijiazhuang ~~and~~, Tianjin, Hebei and Henan, respectively.

Further, the impacts of aerosols-radiation interaction on the forecasts of surface radiation, energy budget, and meteorology parameters were evaluated against surface and sounding observations. The results showed that the decrease of downward SW radiation reaching surface induced by aerosol effects helped to reduce the overestimation of SW radiation during daytime. Moreover, the simulated surface radiation budget has also been improved, with the biases of net radiation at surface decreased by 85.3%, 50.0%, 35.4%, and 44.1% during daytime at Beijing, Tianjin, Taiyuan and Jinan respectively, accompanied by the reduction of sensible (16.1 W m^{-2},

18.5%) and latent (6.8 W m^{-2}, 13.4%) heat fluxes emitted by the surface at noon-time.

The energy budget changed by aerosol extinction further cools 2-m temperature by ~0.40°C over NCP, reducing warm bias by ~73.9% and also leading to lower RMSE, particularly during daytime. Since aerosol cools the lower planetary boundary layer and meanwhile warms the high atmosphere, it induced the more stable stratification of the atmosphere and the declination of PBLH by 40–200m (10%–40%) over NCP. Associating with the changes of planetary boundary structure and more stable near-surface atmosphere, the aerosol-radiation interaction tended to weaken the anticyclonic circulation including the east wind over the south part of the domain and northwest wind over the ocean areas. Thus the bias of wind speed over south and northeast part of the domain were decreased particularly during the afternoon, while increased over Beijing and Hebei area. In regard of NCP-average, the overestimated 10m wind speed was improved during whole day with the maximum up to 0.08 m s^{-1} (~7.8%) at 1400LT. The comparison between simulated vertical profiles of atmospheric wind speed with soundings also indicated that Aero was in better agreement with observation and aerosol-radiation interaction helped to improve the prediction of dynamic fields such as atmospheric wind through the thermal wind relation by altering the atmospheric structure.

The impacts of aerosol-radiation interactions on wind field at 850hPa were further discussed. The results showed that aerosol-radiation interaction will prevent pollutants from dispersing and may exacerbate the pollution through changes of both U and V

wind, which confirms the more stable boundary layer due to aerosol-radiation. These wind field changes may also influence the forecast of the transport and dissipation of the pollutants by WRF-Chem through changed meteorological ICs.

This study analyzed the impacts of aerosol-radiation interaction on radiation and meteorological forecast by using the offline-coupling of WRF and high-frequent updated AOD simulated by WRF-Chem, which is more computationally economic than the online simulation with the integration time for 96h forecast of about 40% of that for online simulation. This approach allows for a potential application to include aerosol-radiation interaction in our current operational NWP systems. The results revealed that aerosol-radiation interaction had profound influence on the improvement of predictive accuracy and the potential prospects for its application in regional NWP in northern China. Given that most of these analyses were based on a single case of pollution occurred during the wintertime of 2015, there is clearly a need for further research on more polluted cases to achieve more quantitative results before the operational application. As the simulated AOD was adopted in the present study, it should be noted that there exits a discrepancy between simulated AOD and observation in both spatial distribution and temporal variation, which may influence the impacts of aerosol-radiation interaction. Meanwhile, surface energy budget and atmospheric dynamics are also influenced by aerosol-cloud interaction, which are related to cloud microphysical processes and are not discussed in this study.

Data availability Data are available upon request from the first authors Yang Yang (yyang@ium.cn) and corresponding authors Xiujuan Zhao (xjzhao@ium.cn) and Dan Chen (dchen@ium.cn).

Author contribution Yang Yang, Min Chen, Xiujuan Zhao and Dan Chen designed the experiments, Yang Yang and Xiujuan Zhao performed the simulations and carried them out. Yang Yang and Dan Chen prepared the manuscript with contributions from all co-authors.

Competing interests The authors declare that they have no conflict of interest.

Acknowledgments This work was jointly supported by the National Key R&D Program of China (grant nos. 2017YFC1501406 and 2018YFF0300102), Natural Science Foundation of Beijing Municipality (8161004), the National Natural Science Foundation of China (grant nos. 41705076, 41705087 and 41705135~~) and~~), Beijing Major Science and Technology Project (Z181100005418014~~).~~) and Beijing Natural Science Foundation (grant no. 8204074).

Reference

Ackerman, A. S., Toon, O. B., Stevens, D. E., Heymsfield, A. J., Ramanathan, V., and Welton, E. J.: Reduction of tropical cloudiness by soot, Science, 288, 1042–1047, https://doi.org/10.1126/science.288.5468.1042, 2000.

Baklanov, A., Schlünzen, K., Suppan, P., Baldasano, J., Brunner, D., Aksoyoglu, S., Carmichael, G., Douros, J., Flemming, J., Forkel, R., Galmarini, S., Gauss, M., Grell, G., Hirtl, M., Joffre, S., Jorba, O., Kaas, E., Kaasik, M., Kallos, G., Kong, X., Korsholm, U., Kurganskiy, A., Kushta, J., Lohmann, U., Mahura, A., Manders-Groot, A., Maurizi, A., Moussiopoulos, N., Rao, S. T., Savage, N., Seigneur, C., Sokhi, R. S., Solazzo, E., Solomos, S., Sørensen, B., Tsegas, G., Vignati, E., Vogel, B., and Zhang, Y.: Online coupled regional meteorology chemistry models in Europe: current status and prospects, Atmos. Chem. Phys., 14, 317–398, https://doi.org/10.5194/acp-14-317-2014, 2014.

Chan, C. K. and Yao, X.: Air pollution in mega cities in China, Atmos. Environ., 42, 1–42, https://doi.org/10.1016/j.atmosenv.2007.09.003, 2008.

Chen, D., Liu, Z., Davis, C., and Gu, Y.: Dust radiative effects on atmospheric thermodynamics and tropical cyclogenesis over the Atlantic Ocean using WRF-Chem coupled with an AOD data assimilation system, Atmos. Chem. Phys., 17, 7917–7939, https://doi.org/10.5194/acp-17-7917-2017, 2017.

Chen, F. and Dudhia, J.: Coupling an advanced land surface-hydrology model with the Penn State-NCAR MM5 modeling system. Part I: Model implementation and

sensitivity, Mon. Wea. Rev., 129, 569–585, doi: 10.1175/1520-0493(2001)129<0569:CAALSH>2.0.CO;2, 2001.

Cheng, X., Sun, Z., Li, D., Xu, X., Jia, M., and Cheng, S.: Short-term aerosol radiative effects and their regional difference during heavy haze episodes in January 2013 in China, Atmos. Environ., 165, 248–263, http://dx.doi.org/10.1016/j.atmosenv.2017.06.040, 2017.

Cheng, Y. F., Eichler, H., Wiedensohler, A., Heintzenberg, J., Zhang, Y. H., Hu, M., Herrmann, H., Zeng, L.M., Liu, S., Gnauk, T., Brüggemann, E., and He, L.Y., Mixing state of elemental carbon and non-light-absorbing aerosol components derived from in situ particle optical properties at Xinken in Pearl River Delta of China, J. Geophys. Res.-Atmos.,111, D20204, doi: 10.1029/2005JD006929, 2006.

Chou, M. D. and Suarez, M. J.: A solar radiation parameterization for atmospheric studies, Tech. Rep. NASA/TM-1999-104606, 15, Technical Report Series on Global Modeling and Data Assimilation NASA, 1999.

Ek, M. B., Mitchell, K. E., Lin, Y., Rogers, E., Grunmann, P., Koren, V., Gayno, G., and Tarpley, J.D.: Implementation of Noah land surface model advances in the National Centers for Environmental Prediction operational mesoscale Eta model, J. Geophys. Res.-Atmos, 108, 8851, doi:10.1029/2002JD003296, 2003.

Elser, M., Huang, R.-J., Wolf, R., Slowik, J. G., Wang, Q., Canonaco, F., Li, G., Bozzetti, C., Daellenbach, K. R., Huang, Y., Zhang, R., Li, Z., Cao, J., Baltensperger, U., El-Haddad, I., and Prévôt, A. S. H.: New insights into $PM_{2.5}$ chemical composition and

621 sources in two major cities in China during extreme haze events using aerosol mass
622 spectrometry, Atmos. Chem. Phys., 16, 3207–3225, https://doi.org/10.5194/acp-16-
623 3207-2016, 2016.
624 Fan, J., Zhang, R., Tao, W. K., and Mhor, K. I.: Effects of aerosol optical properties on
625 deep convective clouds and radiative forcing, J. Geophys. Res., 113, D08209,
626 doi:10.1029/2007JD009257, 2008.
627 Ghan, S. J., Liu, X., Easter, R. C., Zaveri, R., Rasch, P. J., Yoon, J.-H., Eaton, B.: Toward
628 a Minimal Representation of Aerosols in Climate Models: Comparative
629 Decomposition of Aerosol Direct, Semidirect, and Indirect Radiative Forcing, J.
630 Clim., 2012, 25, 6461-6476, doi: 10.1175/JCLI-D-11-00650.1, 2012.
631 Grell, G. A. and Baklanov, A.: Integrated modelling for forecasting weather and air
632 quality: a call for fully coupled approaches, Atmos. Environ., 45, 6845–6851,
633 https://doi.org/10.1016/j.atmosenv.2011.01.017, 2011.
634 Grell, G. A. and Dévényi, D.: A generalized approach to parameterizing convection
635 combining ensemble and data assimilation techniques, Geophys. Res. Lett., 29, 1693,
636 doi: 10.1029/2002GL015311, 2002.
637 Grell, G., Freitas, S. R., Stuefer, M., and Fast, J.: Inclusion of biomass burning in WRF-
638 Chem: impact of wildfires on weather forecasts, Atmos. Chem. Phys., 11, 5289-5303,
639 https://doi.org/10.5194/acp-11-5289-2011, 2011.
640 Guo, J., Deng, M., Lee, S. S., Wang, F., Li, Z., Zhai, P., Liu, H., Lv, W., Yao, W., and
641 Li, X.,: Delaying precipitation and lightning by air pollution over the pearl river delta.

642 Part I: observational analyses, J. Geophys. Res.-Atmos, 121, 6472–6488,
643 doi:10.1002/2015JD023257, 2016.
644 Hansen, J., Sato, M., and Ruedy, R.: Radiative forcing and climate response, J. Geophys.
645 Res.-Atmos, 102, 6831–6864, https://doi.org/10.1029/96JD03436, 1997.
646 Hong, S.-Y., Noh, Y., and Dudhia, J.: A new vertical diffusion package with an explicit
647 treatment of entrainment processes, Mon. Weather Rev., 134, 2318–2341,
648 doi:10.1175/Mwr3199.1, 2006.
649 Huang, C.-C., Chen, S.-H., Lin, Y.-C., Earl, K., Matsui, T., Lee, H.-H., Tsai, I-C., Chen,
650 J.-P., and Cheng, C.-T.: Impacts of Dust–Radiation versus Dust–Cloud Interactions
651 on the Development of a Modeled Mesoscale Convective System over North Africa,
652 Mon. Weather Rev., 47, 3301-3326. https://doi.org/10.1175/MWR-D-18-0459.1,
653 2019.
654 Huang, X., Ding, A., Liu, L., Liu, Q., Ding, K., Niu, X., Nie, W., Xu, Z., Chi, X., Wang,
655 M., Sun, J., Guo, W., and Fu, C.: Effects of aerosol–radiation interaction on
656 precipitation during biomass-burning season in East China, Atmos. Chem. Phys., 16,
657 10063–10082, https://doi.org/10.5194/acp-16-10063-2016, 2016.
658 Iacono, M. J., Delamere, J. S., Mlawer, E. J., Shephard, M. W., Clough, S. A., Collins,
659 W. D.: Radiative forcing by long-lived greenhouse gases: Calculations with the AER
660 radiative transfer models, J. Geophys. Res.-Atmos,113, D13, doi:
661 10.1029/2008JD009944, 2008.
662 Kain, J. S.: The Kain-Fritsch convective parameterization: An update, J. Appl.

Meteorol., 43, 170–181, 2004.

Kaufman, Y. J., Tanre, D., and Boucher, O.: A satellite view of aerosols in the climate system, Nature, 419, 215-223, http://dx.doi.org/10.1038/nature01091, 2002.

Liao, H., Chen, W. T., and Seinfeld, J. H.: Role of climate change in global predictions of future tropospheric ozone and aerosols, J. Geophys. Res., 111, D12304, doi:10.1029/2005JD006852, 2006.

Liao, L., Lou, S. J., Fu, Y., Chang, W. J., and Liao, H.: Radiative forcing of aerosols andits impact on surface air temperature on the synoptic scale in eastern China, Chinese J. Atmos. Sci. (in Chinese), 39, 68–82.,doi: doi: 10.3878/j.issn.1006-9895.1402.13302, 2015.

Liu, X., Zhang, Y., Cheng, Y., Hu, M., and Han, T.: Aerosol hygroscopicity and its impact on atmospheric visibility and radiative forcing in Guangzhou during the 2006 PRIDE-PRD campaign, Atmos. Environ. 60, 59–67, https://doi.org/10.1016/j.atmosenv.2012.06.016, 2012.

Mlawer, E. J., Taubman, S. J., Brown, P. D., Iacono, M. J. and Clough, S. A.: Radiative transfer for inhomogeneous atmospheres: RRTM, a validated correlated-k model for the longwave, J. Geophys. Res., 102, doi:10.1029/97JD00237. 16663-16682, 1997.

Mulcahy, J. P., Walters, D. N., Bellouin, N., and Milton, S. F.: Impacts of increasing the aerosol complexity in the Met Office global numerical weather prediction model, Atmos. Chem. Phys., 14, 4749–4778, https://doi.org/10.5194/acp-14-4749-2014, 2014.

Oreopoulos, L., Mlawer, E., Delamere, J., Shippert, T., Cole, J., Fomin, B., Iacono, M., Jin, Z., Li, J., Manners, J., Räisä-nen, P., Rose, F., Zhang, Y., Wilson, M. J., and Rossow, W. B.: The Continual Intercomparison of Radiation Codes: Results from Phase I, J. Geophys. Res.-Atmos., 117, D06118, https://doi.org/10.1029/2011JD016821, 2012.

Péré, J. C., Mallet, M., Pont, V., and Bessagnet B.: Impact of aerosol direct radiative forcing on the radiative budget, surface heat fluxes, and atmospheric dynamics during the heat wave of summer 2003 over western Europe: A modeling study, J. Geophys. Res., 116, D23119, https://doi.org/10.1029/2011JD016240, 2011.

Pleim. J. E.: A Combined local and nonlocal closure model for the atmospheric boundary layer. Part I: Model description and testing, J. Appl. Meteorol. Climat., 46, 1383–1395, doi: 10.1175/JAM2539.1, 2007.

Quan, J., Tie, X., Zhang, Q., Liu, Q., Li, X., Gao, Y., and Zhao D.: (2014). Characteristics of heavy aerosol pollution during the 2012–2013 winter in beijing, China, Atmos. Environ., 88, 83-89, https://doi.org/10.1016/j.atmosenv.2014.01.058, 2014.

Ramanathan, V., Crutzen, P. J., Kiehl, J. T., and Rosenfeld, D.: Aerosols, Climate and the Hydrological Cycle, Science, 294, 2119–2124, 2001.

Rémy, S., Benedetti, A., Bozzo, A., Haiden, T., Jones, L., Razinger, M., Flemming, J., Engelen, R. J., Peuch, V. H., and Thepaut, J. N.: Feedbacks of dust and boundary layer meteorology during a dust storm in the eastern Mediterranean, Atmos. Chem.

Phys., 15, 12909–12933, https://doi.org/10.5194/acp-15-12909-2015, 2015.

Rodwell, M. J. and Jung T.: Understanding the local and global impacts of model physics changes: an aerosol example, Q. J. Roy. Meteor. Soc., 134, 1479-1497, https://doi.org/10.1002/qj.298, 2008.

Rogers, R. E., Deng, A. J., Stauffer, D. R., Gaudet, B. J., Jia, Y. Q., Soong, S. T., and Tanrikulu, S.: Application of the Weather Research and Forecasting Model for Air Quality Modeling in the San Francisco Bay Area, J. Appl. Meteor. Clim., 52, 1953–1973, doi: 10.1175/JAMC-D-12-0280.1, 2013.

Ruiz-Arias, J. A., Dudhia, J., and Gueymard, C. A.: A simple parameterization of the short-wave aerosol optical properties for surface direct and diffuse irradiances assessment in a numerical weather model, Geosci. Model Dev., 7, 1159–1174, doi:10.5194/gmd-7-1159-2014, 2014.

Sekiguchi, A., Shimadera, H., and Kondo, A.: 2018, Impact of Aerosol Direct Effect on Wintertime $PM_{2.5}$ Simulated by an Online Coupled Meteorology-Air Quality Model over East Asia, Aerosol and Air Quality Research, 18: 1068–1079, doi: 10.4209/aaqr.2016.06.0282, 2018.

Thompson, G., Field, P. R., Rasmussen, R. M., and Hall, W. D.: Explicit forecasts of winter precipitation using an improved bulk microphysics scheme. Part II: Implementation of a new snow parameterization, Mon. Weather Rev., 136, 5095–5115, https://doi.org/10.1175/2008MWR2387.1, 2008.

Toll, V., Gleeson, E., Nielsen, K.P., Männik, A., Mašek, J., Rontu, L., and Post, P.:

726 Impacts of the direct radiative effect of aerosols in numerical weather prediction over
727 Europe using the ALADIN-HIRLAM NWP system, Atmos. Res., 172-173, 163-173,
728 https://doi.org/10.1016/j.atmosres.2016.01.003, 2016.
729 Toll, V., Reis. K., Ots, R., Kaasik, M., Männik, A., Prank, M., Sofiev, M.: SILAM and
730 MACC reanalysis aerosol data used for simulating the aerosol direct radiative effect
731 with the NWP model HARMONIE for summer 2010 wildfire case in Russia, Atmos.
732 Environ., 121, 75-85, https://doi.org/10.1016/j.atmosenv.2015.06.007, 2015.
733 Wang, H., Shi, G. Y., Zhang, X. Y., Gong, S. L., Tan, S. C., Chen, B., Che, H. Z., and
734 Li, T.: Mesoscale modelling study of the interactions between aerosols and PBL
735 meteorology during a haze episode in China Jing–Jin–Ji and its near surrounding
736 region – Part 2: Aerosols' radiative feedback effects, Atmos. Chem. Phys., 15, 3277-
737 3287, https://doi.org/10.5194/acp-15-3277-2015, 2015b.
738 Wang, H., Xue, M., Zhang, X. Y., Liu, H. L., Zhou, C. H., Tan, S. C., Che, H. Z., Chen,
739 B., and Li, T.: Mesoscale modeling study of the interactions between aerosols and
740 PBL meteorology during a haze episode in Jing–Jin–Ji (China) and its nearby
741 surrounding region – Part 1: Aerosol distributions and meteorological features,
742 Atmos. Chem. Phys., 15, 3257–3275, https://doi.org/10.5194/acp-15-3257-2015,
743 2015a.
744 Wang, J., Wang, S., Jiang, J., Ding, A., Zheng, M., Zhao, B., Wong, D. C., Zhou, W.,
745 Zheng, G., Wang, L., Pleim, J. E. and Hao, J.: Impact of aerosol–meteorology
746 interactions on fine particle pollution during China's severe haze episode in January

2013, Environ. Res. Lett., 9, 094002, doi:10.1088/1748-9326/9/9/094002, 2014.

Wang, X, He, X., Miao, S., Dou, Y.: Numerical simulation of the influence of aerosol radiation effect on urban boundary layer, Sci. China Earth Sci., 61, 1844–1858, https://doi.org/10.1007/s11430-018-9260-0, 2018.

Yang, X., Zhao, C., Zhou, L., Wang, Y., Liu, X.: Distinct impact of different types of aerosols on surface solar radiation in China, J. Geophys. Res.-Atmos., 121, 6459-6471, doi: 10.1002/2016JD024938, 2017b.

Yang, Y. and Ren, R. C.: On the contrasting decadal changes of diurnal surface temperature range between the Tibetan Plateau and southeastern China during the 1980s–2000s, Adv. Atmos. Sci., 34, 181–198, doi: 10.1007/s00376-016-6077-z, 2017a.

Yu, H., Kaufman, Y. J., Chin, M., Feingold, G., Remer, L. A., Anderson, T. L., Balkanski, Y., Bellouin, N., Boucher, O., Christopher, S., DeCola, P., Kahn, R., Koch, D., Loeb, N., Reddy, M. S., Schulz, M., Takemura, T., and Zhou, M.: A review of measurement-based assessments of the aerosol direct radiative effect and forcing, Atmos. Chem. Phys., 6, 613-666, https://doi.org/10.5194/acp-6-613-2006, 2006.

Zaveri, R. A. and Peters, L. K.: A new lumped structure photochemical mechanism for large-scale applications, J. Geophys. Res., 104, 30387–30415, https://doi.org/10.1029/1999JD900876,1999.

Zhai, S., Jacob, D. J., Wang, X., Shen, L., Li, K., Zhang, Y., Gui, K., Zhao, T., and Liao, H.: Fine particulate matter ($PM_{2.5}$) trends in China, 2013–2018: separating

768 contributions from anthropogenic emissions and meteorology, Atmos. Chem. Phys.,
769 19, 11031-11041, https://doi.org/10.5194/acp-19-11031-2019, 2019.
770 Zhang, B., Wang, Y., and Hao, J.: Simulating aerosol–radiation–cloud feedbacks on
771 meteorology and air quality over eastern China under severe haze conditionsin
772 winter, Atmos. Chem. Phys., 15, 2387-2404, https://doi.org/10.5194/acp-15-2387-
773 2015, 2015.
774 Zhang, Q., Ma, Q., Zhao, B., Liu, X., Wang, Y., Jia, B., and Zhang, X.: Winter haze
775 over North China Plain from 2009 to 2016: Influence of emission and meteorology,
776 Environ. Pollut., 242, 1308–1318. doi:10.1016/j.envpol.2018.08.019, 2018.
777 Zhang, Q., Quan, J., Tie, X., Li, X., Liu, Q., Gao, Y., and Zhao, D. L.: Effects of
778 meteorology and secondary particle formation on visibility during heavy haze events
779 in Beijing, China, Sci. Total Environ., 502, 578–584,
780 https://doi.org/10.1016/j.scitotenv.2014.09.079, 2015.
781 Zhang, Y., Wen, X.-Y., and Jang, C.-J.: Simulating chemistry-aerosol-cloud-radiation-
782 climate feedbacks over the continental U.S. using the online-coupled Weather
783 Research Forecasting Model with chemistry (WRF/Chem), Atmos. Environ. 44,
784 3568–3582, https://doi.org/10.1016/j.atmosenv.2010.05.056, 2010.
785 Zhang, Y.-Z, Miao, S.-G., Dai, Y.-J., Liu, Y.-H., Numerical simulation of characteristics
786 of summer clear day boundary layer in Beijing and the impact of urban underlying
787 surface on sea breeze (in Chinese), Chin J. Geophys, 56, 2558–2573, 2013.
788 Zhao, X., Li, Z., Xu, J.: Modification and performance tests of visibility

parameterizations for haze days, Environ. Sci., 40, 1688-1696 (in Chinese), 2019.

Zheng, Y., Che, H., Xia, X., Wang, Y., Wang, H., Wu, Y., Tao, J., Zhao, H., An, J., Li, L., Gui, K., Sun, T., Li, X., Sheng, Z., Liu, C., Yang, X., Liang, Y., Zhang, L., Liu, C., Kuang, X., Luo, S., You, Y., and Zhang, X.: Five-year observation of aerosol optical properties and its radiative effects to planetary boundary layer during air pollution episodes in North China: Intercomparison of a plain site and a mountainous site in Beijing, Sci. Total Environ., 674, 140–158. https://doi.org/10.1016/j.scitotenv.2019.03.418, 2019.

797 Table 1. The variables, sources, numbers of sites in the domain/NCP and the frequency

798 of chemical and meteorological observations.

Variables	Source of observation	Numbers of sites over the domain/NCP	Frequency	locations
AOD	AERONET	3/3	hourly	black dots in Fig. 1b
AOD	IAP station	1/1	hourly	blue dot in Fig. 1b
AOD	MODIS	/	daily	Fig. 2f-j and Fig. 2p-t
aerosol extinction coefficient	CALIPSO	/	daily	black paths in Fig.3a-d
$PM_{2.5}$	China National Environmental Monitoring Centre	813/332	hourly	dots in Fig. ~~3a~~5a
radiation	China Meteorological Administration	4/4	hourly	triangles in Fig. 1a
radiation	IAP station	1/1	hourly	triangles in Fig. 1a
2-m temperature	China Meteorological Administration	1157/534	hourly	dots in Fig. ~~8a~~11a
wind at 10m	China Meteorological Administration	1157/534	hourly	dots in Fig. ~~8a~~11a
atmospheric wind	China Meteorological Administration	2/2	0800LT, 2000LT	circles in Fig. 1a

799

Table 2. Mean bias of downward SW radiation at surface (W m^{-2}) and Net radiation at surface (W m^{-2}) from NoAero and Aero relative to observation during daytime (averaged 0800 to 1800 LT) and nighttime (averaged 1900 to 0700 LT), averaged from 6th to 11th Dec. 2015 at Beijing, Tianjin, Taiyuan and Jinan respectively.

Station	SW radiation		Net radiation			
	Daytime		Daytime		Nighttime	
	NoAero	Aero	NoAero	Aero	NoAero	Aero
Beijing	149.4	38.0	102.2	15.0	-33.6	-33.2
Tianjin	115.5	70.9	72.2	36.4	-27.1	-26.4
Taiyuan	155.0	118.3	66.9	43.2	-33.6	-33.3
Jinan	149.1	97.7	81.2	45.3	-30.3	-29.3

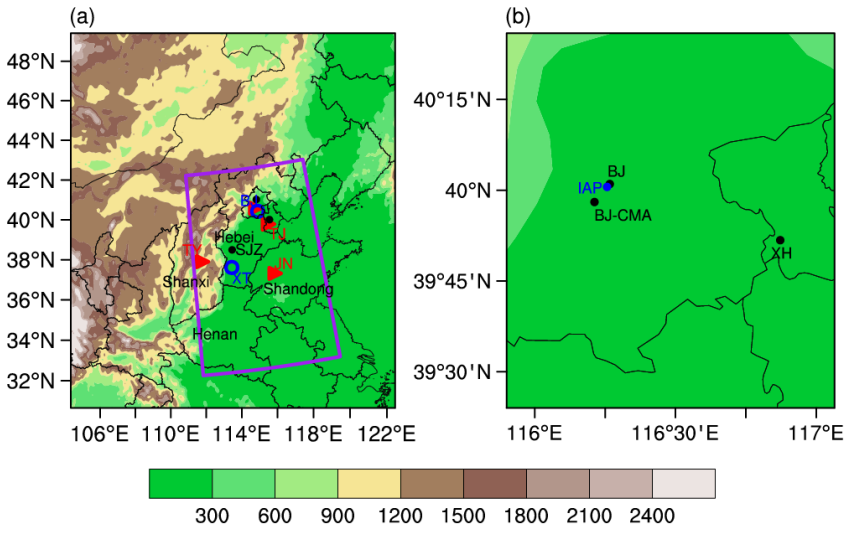

Figure 1. (a) The model domain and the terrain height (shadings, m). Purple box denotes the NCP, triangles are the observational sites of radiation (BJ: Beijing, TJ: Tianjin, TY: Taiyuan and JN: Jinan), circles are sites of sounding observation (BJ: Beijing and XT: Xingtai), dots denote the major cities for validation of $PM_{2.5}$ (BJ: Beijing, SJZ: Shijiazhuang and TJ: Tianjin). Names of provinces are also added (Hebei, Shanxi, Shandong and Henan). (b) The observational sites of AOD, including AERONET sites (black dots, BJ: Beijing, BJ-CMA: Beijing-CMA and XH: Xianghe) and IAP in-situ (blue dot) site.

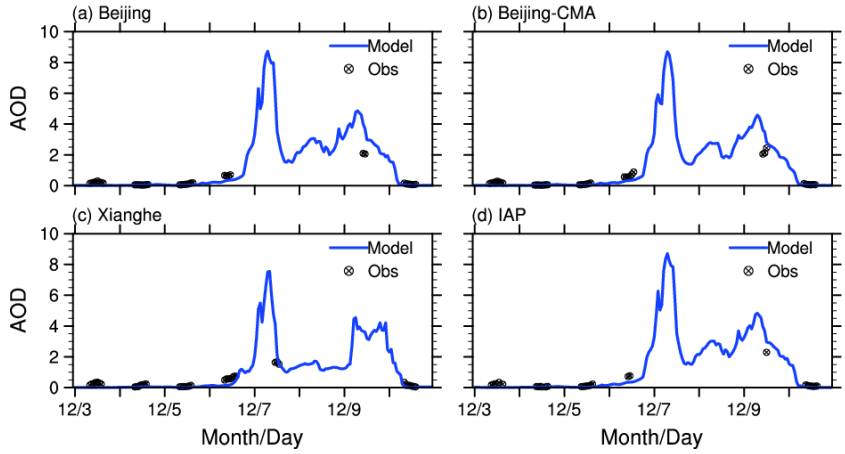
(a) Beijing
(b) Beijing-CMA
(c) Xianghe
(d) IAP
Model
Obs
AOD
0
2
4
6
8
10
12/3
12/5
12/7
12/9
Month/Day

Figure 2.

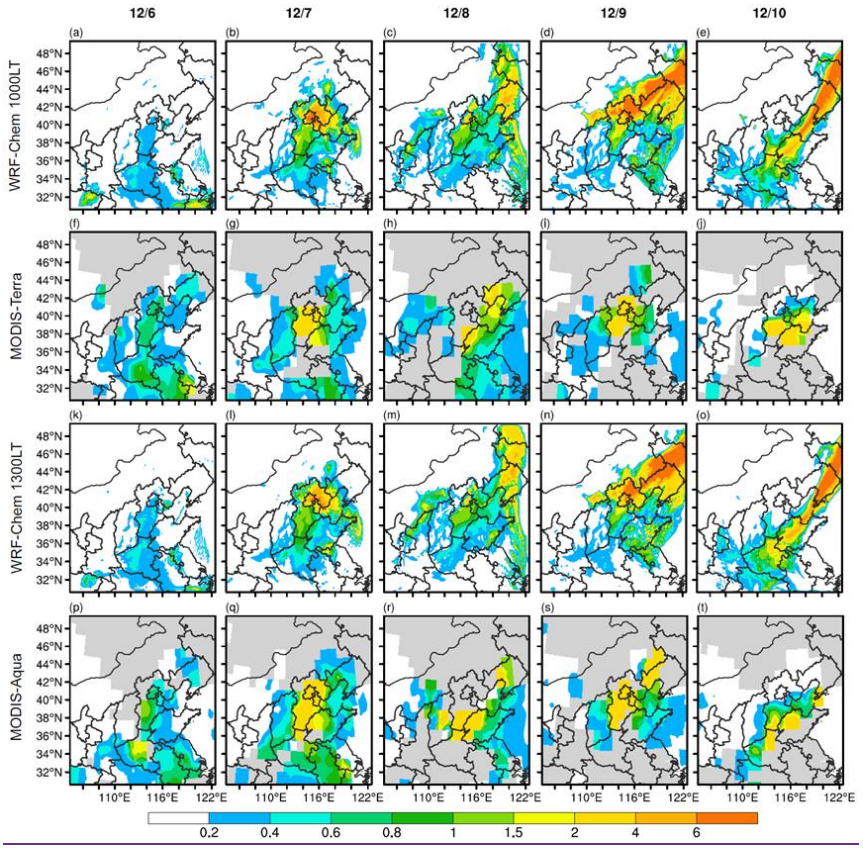

Figure 2. The WRF-Chem simulated and MODIS observed spatial distribution of AOD on 6th-10th December (from left to right). The first (a-e) and third rows (k-o) are WRF-Chem simulations at 1000LT and 1300LT (MODIS path times) respectively. The second (f-j) and fourth (p-t) rows are MODIS Terra and Aqua observations, respectively. Gray areas in (f-j) and (p-t) denote the missing values.

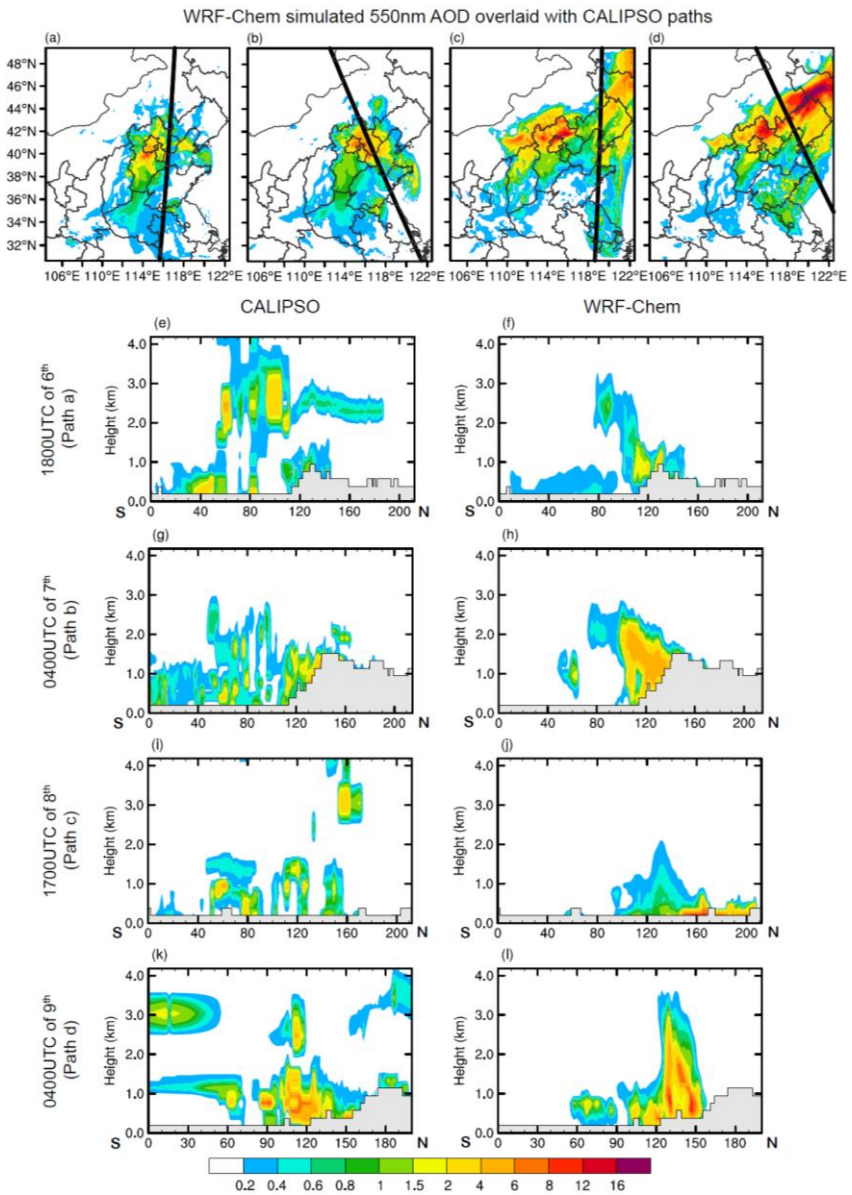

Figure 3. The WRF-Chem simulated 550nm AOD (shadings) on (a)1800UTC of 6th, (b) 0400UTC of 7th, (c)1700UTC of 8th, (d) 0400UTC of 9th December overlaid with CALIPSO paths (black thick solid). (e-l) denote the corresponding vertical distributions

of aerosol extinction coefficient at 550nm from (e, g, i, k) CALIPSO and (f, h, j, l) model simulations. Gray areas in (e-l) denote the terrain.

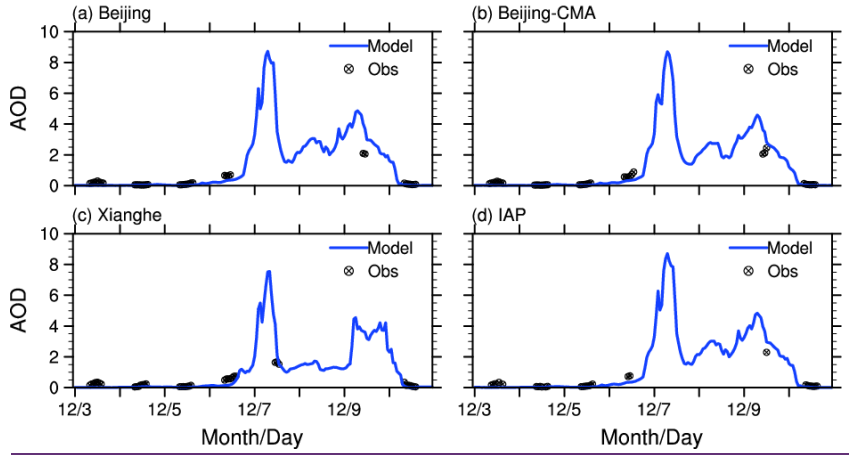

Figure 4. Temporal variation of observed (black dots) and simulated (blue) AOD at 550nm during 3rd-10th Dec. (LT) at (a) Beijing, (b) Beijing-CMA, (c) Xianghe and (d) IAP, AOD observations are from (a-c) AERONET and (d) IAP in-situ site.

834

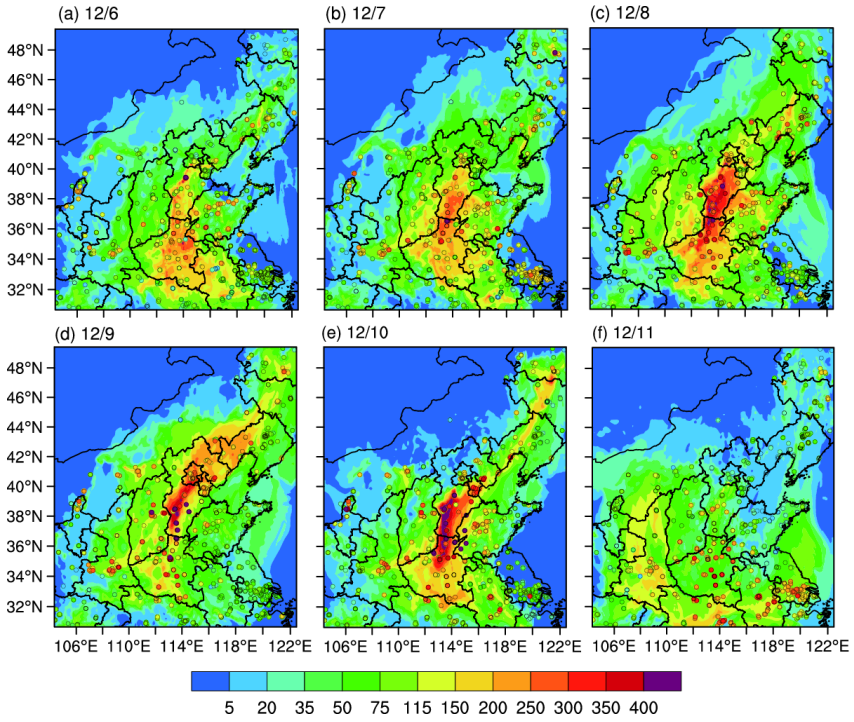

Figure ~~3~~5. Observed (colored dots) and WRF-Chem simulated (shadings) spatial distribution of $PM_{2.5}$ concentrations (μg m^{-3}) on 0800LT of (a) 6th, (b) 7th, (c) 8th, (d) 9th, (e) 10th and (f) 11th Dec. respectively.

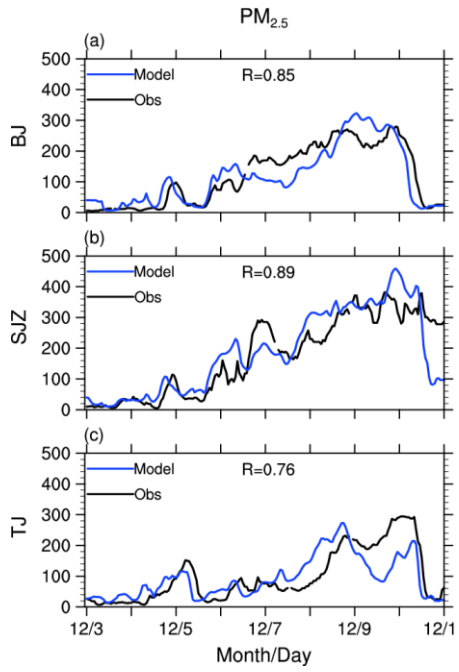
PM2.5
(a)
Model
Obs
R=0.85
BJ
(b)
Model
Obs
R=0.89
SJZ
(c)
Model
Obs
R=0.76
TJ
0
100
200
300
400
500
12/3
12/5
12/7
12/9
12/1
Month/Day

Figure 4.

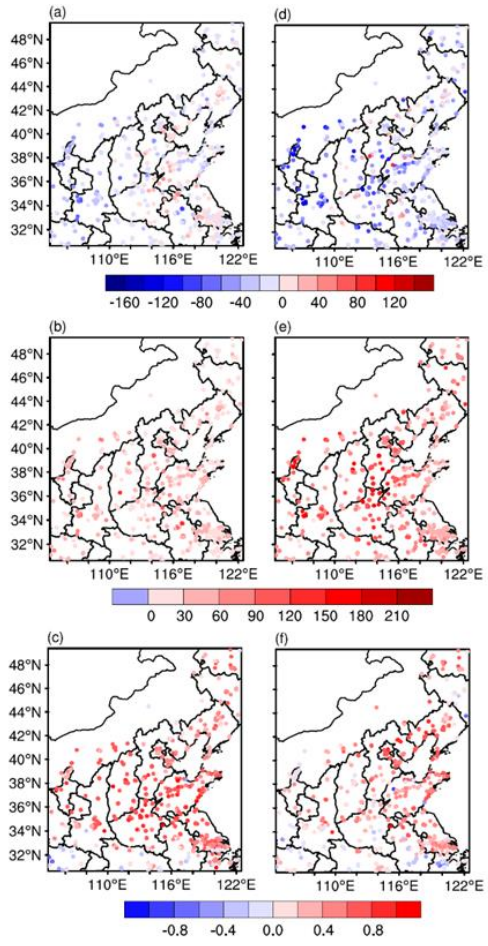

841

842 Figure 6. The (a, d) bias (μg m^{-3}), (b, e) RMSE (μg m−3), and (c, f) correlation

843 coefficient (1) averaged (a-c) during clean period (3th to 5th Dec.) and (d-f) the polluted

844 period (6th to 10th December).

845

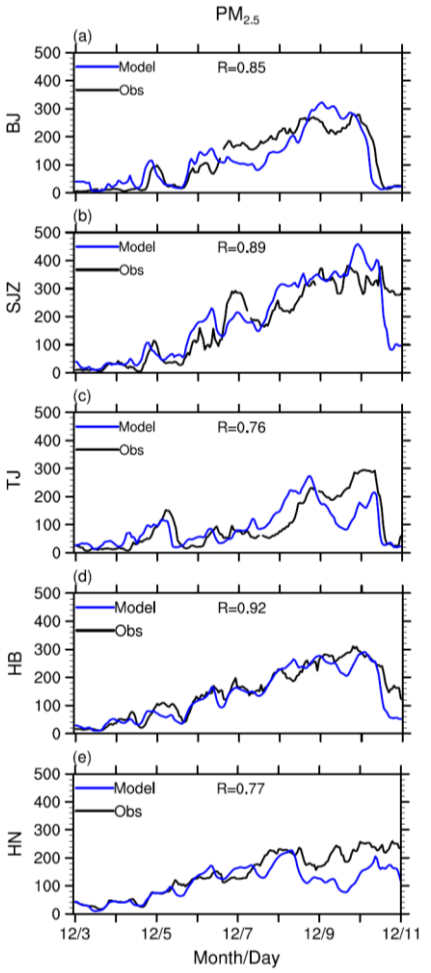

Figure 7. Observed (black) and WRF-Chem simulated (blue) temporal variation of $PM_{2.5}$ ($\mu g\ m^{-3}$) at three major cities~~:~~ (a) Beijing (BJ), (b) Shijiazhuang (SJZ) ~~and~~ (c) Tianjin (TJ)~~.~~

带格式的: 英语(美国)

带格式的: 英语(美国)

带格式的: 英语(美国)

带格式的: 英语(美国)

) and two provinces (d) Hebei (HB) and (e) Henan (HN).

带格式的: 英语(美国)

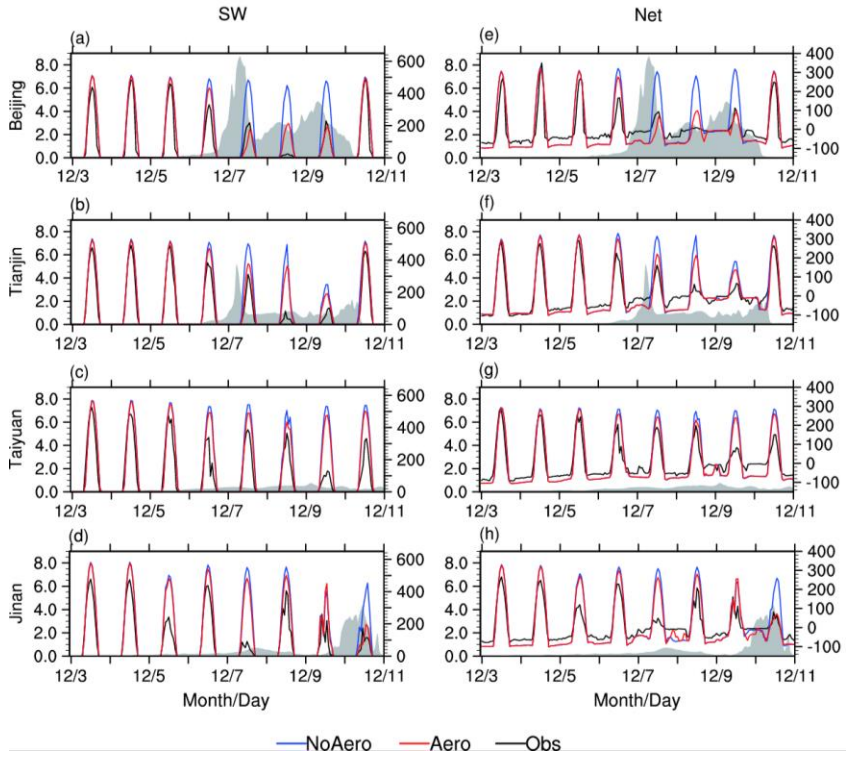

852

853 Figure ~~5~~8. (a–d) observed (black) and WRF simulated (NoAero: blue, Aero: red)

854 temporal variation of downward shortwave radaition at surface (W m^{-2}, right axis) at

855 (a) Beijing, (b) Tianjin, (c) Taiyuan and (d) Jinan, respectively. The grey areas indicate

856 the simulated AOD (left axis) by WRF-Chem. (e–h) are same with (a–d), but for net

857 radaition at surface (W m^{-2}).

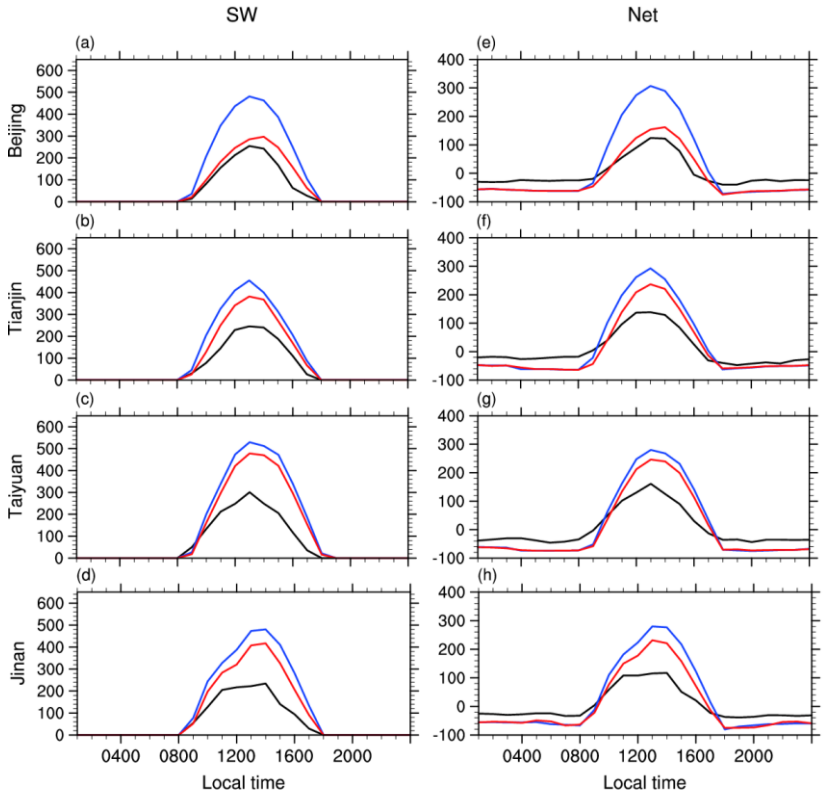
SW
Net
(a)
(b)
(c)
(d)
(e)
(f)
(g)
(h)
Beijing
Tianjin
Taiyuan
Jinan
600
500
400
300
200
100
0
-100
0400
0800
1200
1600
2000
Local time

858

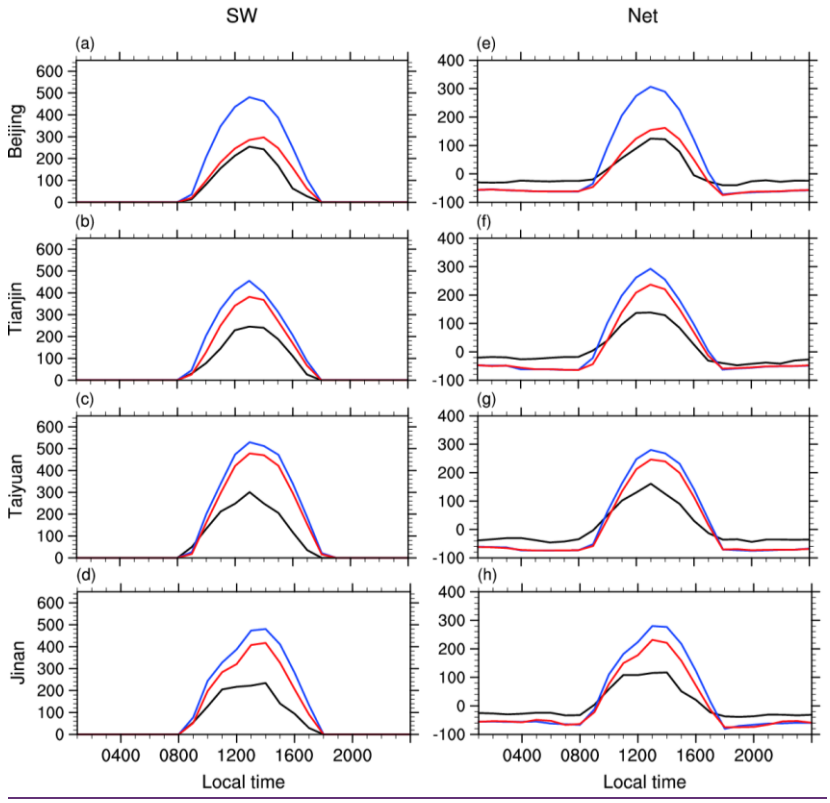

Figure ~~6~~9. (a–d) observed (black) and simulated (NoAero: blue, Aero: red) diurnal cycles of downward shortwave radaition at surface (W m^{-2}) averaged from 6^{th} to 10^{th} Dec. 2015 at (a) Beijing, (b) Tianjin, (c) Taiyuan and (d) Jinan, respectively. (e–h) are same with (a–d), but for net radaition at surface (W m^{-2}).

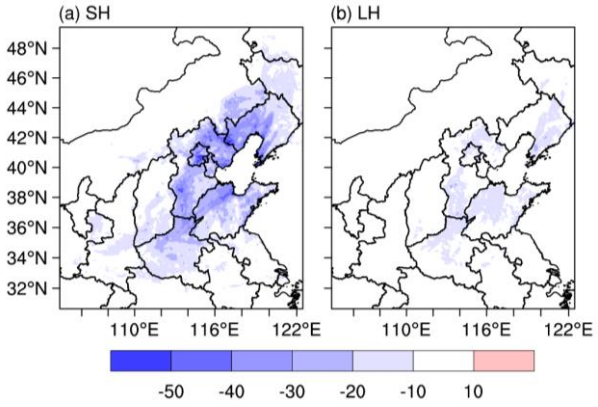

Figure 7<u>10</u>. The differences (Aero minus NoAero) of (a) surface sensible heat flux and (b) surface latent heat flux (W m^{-2}, upward is positive) at 1300LT averaged from 6th to 10th Dec. 2015.

带格式的: 上标

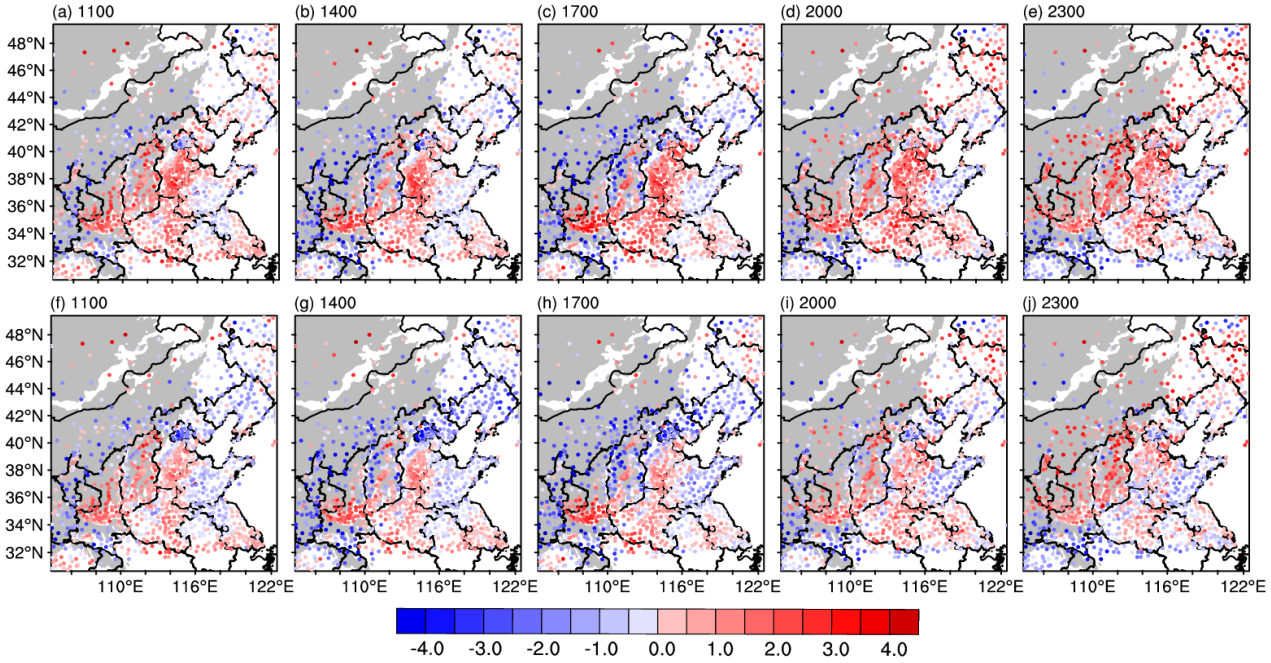

Figure ~~8~~11. The bias of 2-m temperature (°C) at (a) 1100, (b) 1400, (c) 1700, (d) 2000 and (e) 2300 LT in NoAero averaged from 6th to 10th Dec. 2015, (f–j) are same with (a–e), but for Aero. The grey areas denote the areas of terrain height above 1000m.

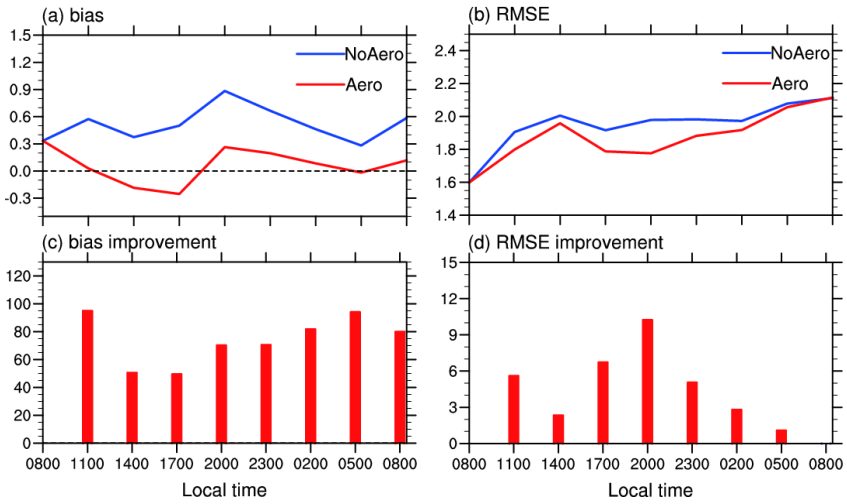

Figure ~~9~~12. Area-averaged (a) bias and (b) RMSE of simulated 2-m temperature (°C) in NoAero (blue) and Aero (red) over NCP area (defined in Fig. 1a), averaged from 6th to 10th Dec. 2015, and the mean improvement (%) of (c) absolute value of bias and (d) RMSE in Aero relative to NoAero.

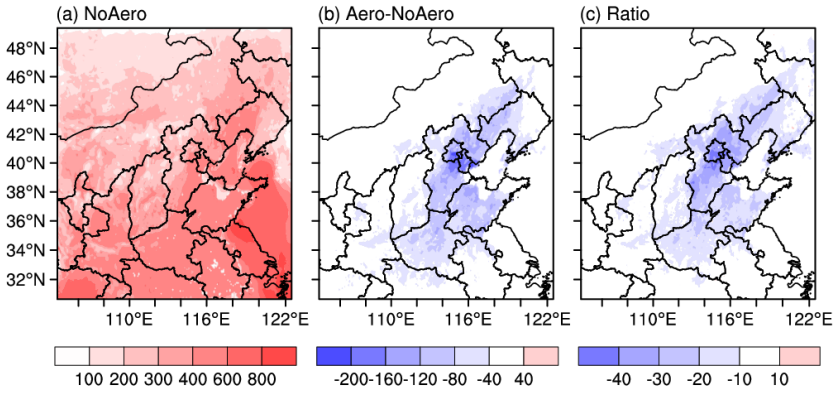

Figure ~~10~~13. Daytime mean PBLH (m) in NoAero, (b) the difference between Aero and NoAero (Aero minus NoAero) and (c) the ratio of changes (%) averaged during 6th to 10th Dec. 2015.

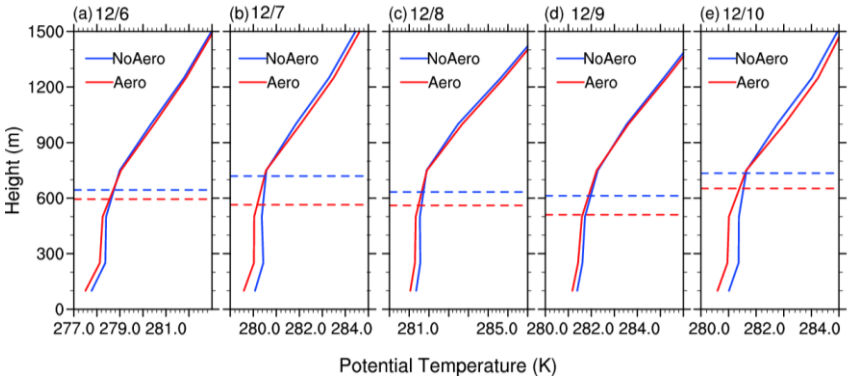

Figure ~~1~~14. NCP (defined in Fig. 1a) area-averaged vertical profiles of potential temperature (K, solid) and planetary boundary-layer height (m, dash) in NoAero (blue) and Aero (red) at 1400 LT of (a) 6th, (b) 7th, (c) 8th, (d) 9th and (e) 10th Dec. 2015.

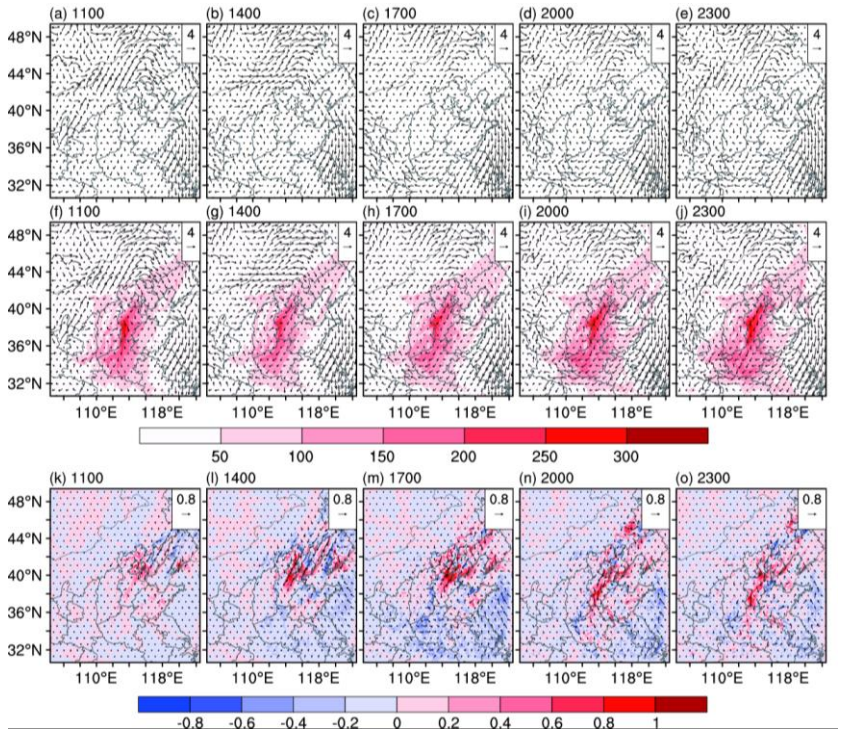

884

885 Figure ~~12~~15. The 10m wind (vector) at 1100, 1400, 1700, 2000 and 2300 LT in (a–e)

886 NoAero and (f–j) Aero averaged during 6th to 10th Dec. 2015, shadings in (f–j) are

887 simulated $PM_{2.5}$ concentrations (μg m^{-3}). (k–o) the difference of 10m wind (vector) and

888 wind speed (shadings) between Aero and NoAero (Aero minus NoAero).

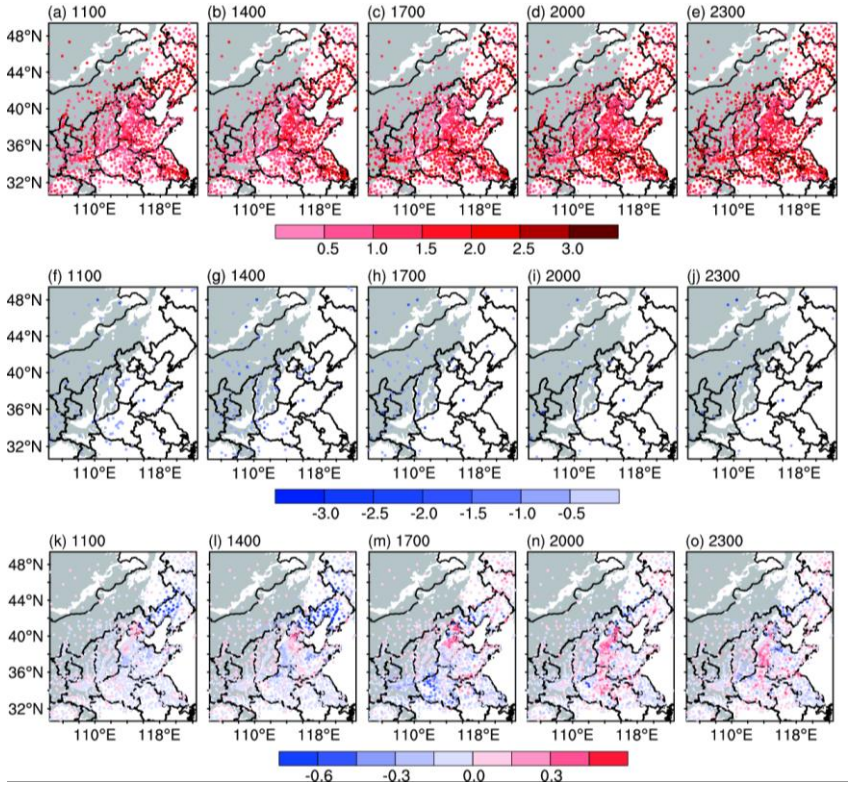

Figure ~~13~~16. The bias of 10m wind speed (m s^{-1}) at 1100, 1400, 1700, 2000 and 2300 LT for (a–e) overestimated sites and (f–j) underestimated sites in NoAero averaged during 6th to 10th Dec. 2015. (k–o) the difference of absolute value of bias (m s^{-1}) between Aero and NoAero (Aero minus NoAero). The grey areas denote the areas of terrain height above 1000m.

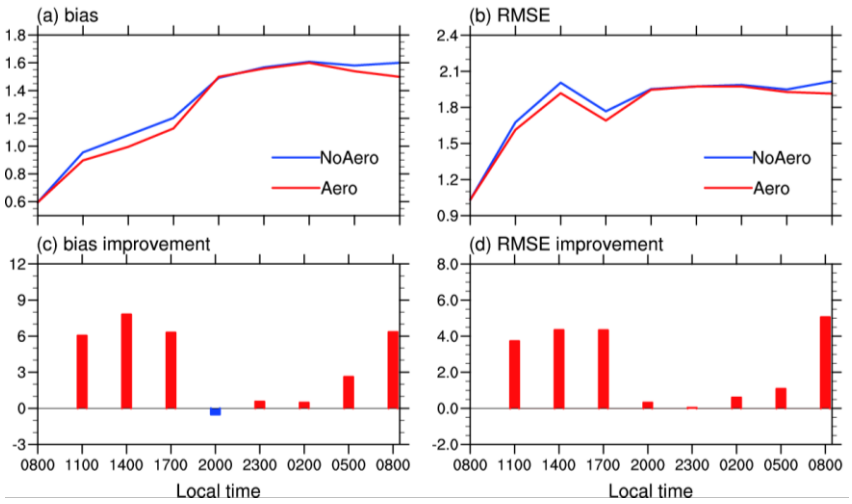

Figure ~~14~~17. Same with Fig.~~9~~12, but for wind speed at 10m (m s $^{-1}$).

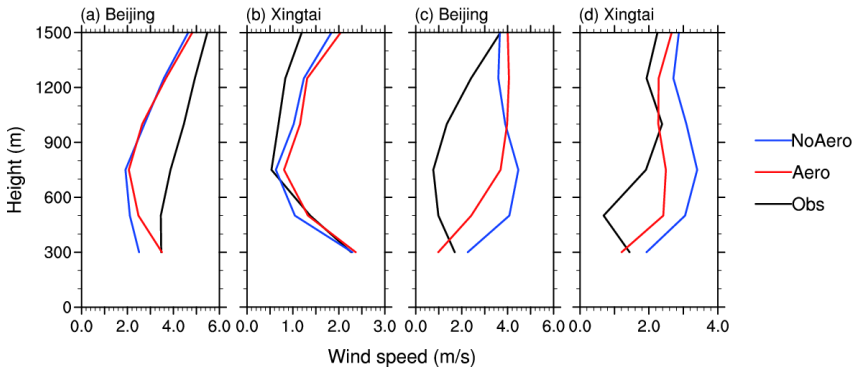

Figure ~~15~~18. (a–b) Observed (black) and simulated (NoAero: blue, Aero: red) vertical profiles of atmospheric wind speed (m s^{-1}) at (a) Bejing and (b)Xingtai at 0800LT averaged from 6th to 10th Dec., (c–d) are same with (a–b), but at 2000LT.

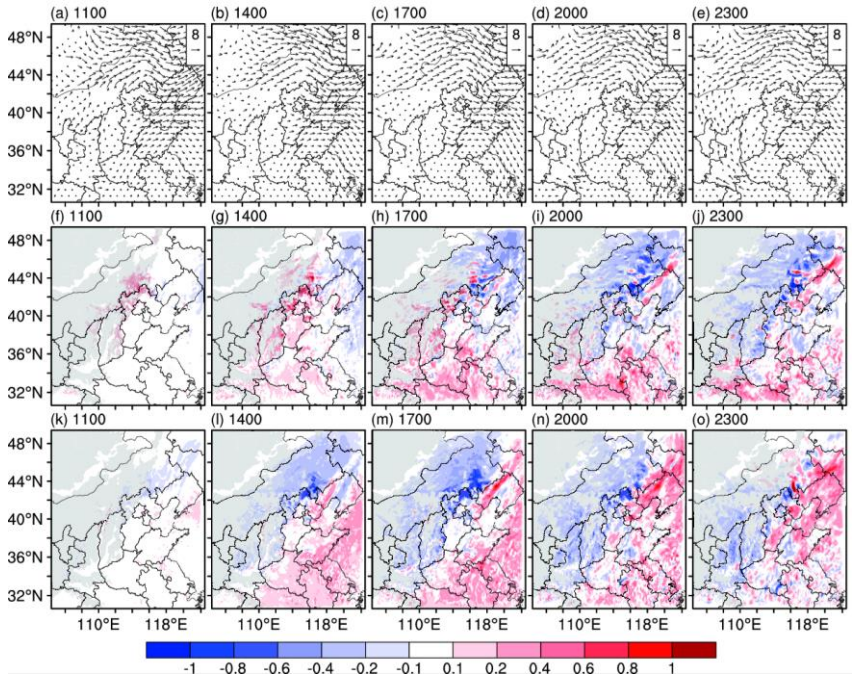

Figure ~~16~~19. The wind at 850hPa (vector) at 1100, 1400, 1700, 2000 and 2300 LT in NoAero averaged during 6th to 10th Dec. 2015. The difference of (f–j) U and (k–o) V wind speed between Aero and NoAero (Aero minus NoAero). The grey areas denote the areas of terrain height above 1000m.